

AD-A102 595

OKLAHOMA UNIV NORMAN SCHOOL OF AEROSPACE MECHANICAL --ETC F/G 13/13
STATIC AND DYNAMIC ANALYSES OF THICK BEAMS OF BIMODULAR MATERIAL--ETC(U)
JUL 81 C W BERT, A D TRAN N00014-78-C-0647
UNCLASSIFIED NL
OU-AMNE-81-7

1 OF 1
AD-A
102595

END
DATE FILED
9-81
DTIC

AD A102595

LEVEL ✓

12

Department of the Navy
OFFICE OF NAVAL RESEARCH
Structural Mechanics Program
Arlington, Virginia 22217

Contract N00014-78-C-0647

Project NR 064-609

Technical Report No. 22

14
Report DU-AMNE-81-7

6
1 STATIC AND DYNAMIC ANALYSES OF
THICK BEAMS OF BIMODULAR MATERIALS.

by

15 Charles W. Bert and A.D. Tran

DTIC
ELECTED
AUG 7 1981
S C

10 Jul 1981

12 72

DTIC FILE COPY

School of Aerospace, Mechanical and Nuclear Engineering
University of Oklahoma
Norman, Oklahoma 73019

Approved for public release; distribution unlimited

1 818 0.018

PART I

BENDING OF THICK BEAMS OF BIMODULUS MATERIALS

A.D. Tran
Exxon Production Research
Houston, Texas

and

C.W. Bert
University of Oklahoma
Norman, Oklahoma

Abstract - The literature on bending of beams made of bimodulus materials (which have one value of the elastic modulus in tension and another in compression) is limited. All of the works known to the present investigators are restricted to beams with natural boundary conditions and subjected to specific distributions of normal pressure only. In the present work, the transfer-matrix approach is used to determine the small-deflection static behavior of bimodulus beams, including transverse shear deformation. The neutral surface, i.e., the locus of points having zero axial normal strain, may vary linearly within each element. The effects of axial load and non-natural boundary conditions are considered. As a basis for comparative evaluation, exact closed-form solutions are also presented for special cases in which the neutral-surface location is constant along the beam axis. Results are compared between the two solution methods and are found to give good agreement.

INTRODUCTION

As early as 1864, St. Venant [1] recognized that certain actual materials have different elastic behavior when they are loaded in tension as compared to compression. See also [2-4]. However, the concept of a bimodulus material,

i.e., a bilinear material having different moduli in tension and in compression was not originated until 1941 by Timoshenko [3], who considered the flexural stresses in such a material undergoing pure bending. The effective modulus for stiffness of such a beam in pure bending was given by Marin [3]. The bimodulus concept was rediscovered and extended to two-dimensional materials by Ambartsumyan [6] in 1965. Subsequently, there have been many analyses of two-dimensional bimodulus material, but this topic is beyond the scope of the present work.

Work analogous to that of Timoshenko [3] or Marin [5] on static, small-deflection bending of Bernoulli-Euler beams of homogeneous, bimodulus material was presented in [7-15]. A so-called no-tension material, which has no resistance to tension but a finite elastic resistance to compression, is a special case of bimodulus material applicable to brittle materials, such as many ceramic materials. Buckling of columns of no-tension material was analyzed in [16-18]. Column buckling of general bimodulus material was considered in [19,20]. Large static deflections of beams of bimodulus material were treated in [21,22]. Transverse shear effects on bimodulus beams were first treated by Kamiya [23]. Bimodulus action in viscoelastic beams was considered by Nachlinger and Leininger [24].

Special studies applicable to bending of specific kinds of nonhomogeneous-material beams were carried out by some investigators. For example, Vierling and Scheele [25] were concerned with cord-rubber, Bilida [26] and Phan-Thien [27] with fiber composites, Carlsson et al. [28] with paperboard, Swift [29] with reinforced concrete, and [30-33] with laminates.

The present work is believed to be the first, in the context of bimodulus beams, in the following respects:

1. Consideration of complicated and concentrated loadings, the latter causing the neutral-surface location (and thus the beam stiffnesses) to change along the length of the beam.
2. Application of the transfer-matrix method.

GOVERNING EQUATIONS FOR SMALL DEFLECTIONS OF A BIMODULUS
BEAM ACCOUNTING FOR TRANSVERSE SHEAR

Consider a beam of thickness h and length ℓ . The origin of a Cartesian coordinate system is located on the central axis with the z -axis being normal to the central axis (see Fig. 1). The stress resultants and stress moment, each per unit width, are defined as:

$$(N, Q) = \int_{-h/2}^{h/2} (\sigma_x, \tau_{xz}) dz \quad ; \quad M = \int_{-h/2}^{h/2} z \sigma_x dz \quad (1)$$

where σ_x and τ_{xz} are respectively the axial normal stress and the transverse shear stress. The theory developed by Yang, Norris, and Stavsky [34] assumes the following displacement field:

$$U(x, z) = u(x) + z\psi(x) \quad ; \quad W(x, z) = w(x) \quad (2)$$

where U and W are the displacement components in the x and z directions, respectively, u and w are the corresponding displacements at the midplane, and ψ is the bending slope,

The constitutive relation for a bimodulus beam with provision for a shift of the neutral surface (due to different properties in tension and compression) can be written as follows [35]:

$$\begin{aligned} \begin{Bmatrix} N \\ M \end{Bmatrix} &= \begin{bmatrix} A & B \\ B & D \end{bmatrix} \begin{Bmatrix} u, x \\ \psi, x \end{Bmatrix} \\ Q &= S(w, x + \psi) \end{aligned} \quad \begin{array}{l} \text{Accession For} \\ \text{NTIS CRA&I} \\ \text{2013} \\ \text{Advanced} \\ \text{Application} \\ \text{By} \\ \text{Distribution/} \\ \text{Availability Codes} \\ \text{11 and/or} \\ \text{Special} \\ \text{111} \end{array} \quad (3)$$

Here, differentiation is denoted by a comma, i.e., $(\cdot)_x \equiv d(\cdot)/dx$. The symbols A, B, D, S denote the respective extensional, flexural-extensional coupling, flexural, and thickness shear stiffnesses defined by

$$(A, B, D) = \int_{-h/2}^{h/2} Q^{(k)}(1, z, z^2) dz ; \quad S = K^2 \int_{-h/2}^{h/2} G^{(k)} dz \quad (k = t, c) \quad (4)$$

The quantity K^2 is a shear correction coefficient which is generally taken to be $5/6$ for static loading of rectangular-section beams; $Q^{(k)}$ is $E_1^{(k)}$ for a compact-section beam or $E_1^{(k)} / (1 - v_{12}^{(k)} v_{21}^{(k)})$ for a wide, thin beam; $G^{(k)}$ is the longitudinal-transverse shear modulus; and $k = t$ for tensile-strain regions or $k = c$ for compressive-strain regions.

One can write the equations of equilibrium as follows:

$$N_x = 0 ; \quad Q_x = -q(x) ; \quad M_x - Q = 0 \quad (5)$$

Here, $q(x)$ is the transverse distributed loading.

Substituting eqns (3) into eqns (5), we obtain the following equations of equilibrium in terms of generalized displacements

$$\begin{aligned} (Au_x + B\psi_x)_x &= 0 \\ [S(w_x + \psi)]_x &= -q(x) \\ (Bu_x + D\psi_x)_x - S(w_x + \psi) &= 0 \end{aligned} \quad (6)$$

The expression for neutral-surface location [36], z_n , can be written as:

$$\epsilon_x = u_{,x} + z_n \psi_{,x} = 0$$

or

$$z_n = -u_{,x}/\psi_{,x} \quad (7)$$

ANALYSIS: CLASSICAL APPROACH

For cases when the neutral-surface locations are constant along the beam axis (x-direction), eqns (6) become

$$\begin{aligned} Au_{xx} + B\psi_{xx} &= 0 \\ A(w_{xx} + \psi_x) &= -q(x) \\ Bu_{xx} + D\psi_{xx} - S(w_x + \psi) &= 0 \end{aligned} \quad (8)$$

Eqns (8) constitute a sixth-order system of linear ordinary differential equations with constant coefficients. The general solution can be written as [37]:

$$\begin{aligned} u(x) &= d_1 + d_2x + \frac{3B}{A} c_4x^2 + u_p \\ \psi(x) &= -c_2 + \frac{6(B^2 - AD)}{SA} c_4 - 2c_3x - 3c_4x^2 + \psi_p \\ w(x) &= c_1 + c_2x + c_3x^2 + c_4x^3 + w_p \end{aligned} \quad (9)$$

where c_1, c_2, c_3, c_4 are arbitrary constants and u_p, ψ_p, w_p are particular solutions. The arbitrary constants are determined by the boundary conditions of the beam at $x = 0$ and $x = \ell$.

The clamped boundary conditions at $x = 0$ and $x = \ell$ are given as

$$u(0) = u(\ell) = 0 \quad ; \quad \psi(0) = \psi(\ell) = 0 \quad ; \quad w(0) = w(\ell) = 0 \quad (10)$$

The clamped boundary conditions at $x = 0$ and free boundary conditions at $x = \ell$ are given as

$$u(0) = N(\ell) = 0 \quad ; \quad \psi(0) = M(\ell) = 0 \quad ; \quad w(0) = Q(\ell) = 0 \quad (11)$$

The values of constants $c_1, c_2, c_3, c_4, d_1, d_2$ for the clamped-clamped and clamped-free boundary conditions are as follows:

For clamped-clamped conditions, the values are:

$$\begin{aligned}
 c_1 &= w_p(0) \quad ; \quad c_2 = \frac{6(B^2 - AD)}{SA} c_4 + \psi_p(0) \\
 c_4 &= \left[\frac{SA}{SA\ell^2 - 12(B^2 - AD)} \right] \psi_p(0) + \psi_p(\ell) - \frac{2}{\ell} [w_p(0) - w_p(\ell)] \\
 c_3 &= \frac{1}{2\ell} [\psi_p(\ell) - \psi_p(0) - 3c_4\ell^2] \quad ; \quad d_1 = -u_p(0) \\
 d_2 &= \frac{1}{\ell} [u_p(0) - u_p(\ell) - \frac{3B}{A} c_4\ell^2]
 \end{aligned} \tag{12}$$

For clamped-free conditions, the values are:

$$\begin{aligned}
 c_1 &= -w_p(0) \quad ; \quad d_1 = -u_p(0) \quad ; \quad c_2 = -w_{p,x}(\ell) - \psi_p(\ell) - \psi_p(0) \\
 c_4 &= \frac{SA}{6(B^2 - AD)} [c_2 - \psi_p(0)] \\
 d_2 &= \frac{1}{B^2 - AD} \{ -B^2 u_{p,x}(\ell) - BD\psi_{p,x}(\ell) + SB\ell[w_{p,x}(\ell) + \psi_p(\ell)] \\
 &\quad + ADu_{p,x}(\ell) + BD\psi_{p,x}(\ell) \} \\
 c_3 &= \frac{1}{2(B^2 - AD)} \{ -ABu_{p,x}(\ell) - AD\psi_{p,x}(\ell) + AS\ell[w_{p,x}(\ell) + \psi_p(\ell)] \\
 &\quad + ABu_{p,x}(\ell) + B^2\psi_{p,x}(\ell) \}
 \end{aligned} \tag{13}$$

The particular solutions for uniform and sinusoidal normal load are as follows:

For uniform normal load $q(x) = q_0$, the particular solutions are

$$\begin{aligned}
 u_p(x) &= \frac{Bq_0}{6(AD - B^2)} x^3 \quad ; \quad \psi_p(x) = -\frac{q_0}{S} x - \frac{Aq_0}{6(AD - B^2)} x^3 \\
 w_p(x) &= \frac{Aq_0}{AD - B^2} x^4
 \end{aligned} \tag{14}$$

For normal load $q(x) = q_0 \sin \alpha x$, the particular solutions are

$$\begin{aligned}
 u_p(x) &= \frac{Bq_0}{\alpha^3(AD - B^2)} \cos \alpha x \\
 \psi_p(x) &= - \frac{Aq_0}{\alpha^3(AD - B^2)} \cos \alpha x \\
 w_p(x) &= \frac{q_0}{\alpha^2} \left[\frac{1}{S} + \frac{A}{\alpha^2(AD - B^2)} \right] \sin \alpha x
 \end{aligned} \tag{15}$$

For normal load $q(x) = q_0 \cos \alpha x$, the particular solutions are

$$\begin{aligned}
 u_p(x) &= - \frac{Bq_0}{\alpha^3(AD - B^2)} \sin \alpha x \\
 \psi_p(x) &= \frac{Aq_0}{\alpha^3(AD - B^2)} \sin \alpha x \\
 w_p(x) &= \frac{q_0}{\alpha^2} \left[\frac{1}{S} + \frac{A}{\alpha^2(AD - B^2)} \right] \cos \alpha x
 \end{aligned} \tag{16}$$

ANALYSIS: TRANSFER-MATRIX APPROACH

A common type of system occurring in engineering practice consists of a number of elements linked together end to end in the form of a chain. Well-known examples are continuous beams, turbine-generator shafts, etc. The transfer-matrix approach is ideally suited to such systems because only successive matrix multiplications are necessary to fit the elements together.

In the transfer-matrix techniques [38,39], the beam is divided into N_s elements of mass m and each mass m is assumed to be concentrated at the mass center of the element. The locations of these point masses are referred to as stations. Consecutive stations are separated by massless fields which contain all of the stiffnesses of the system. Consequently, the model of the beam shown in Fig. 2 consists of two half fields, $\Delta\ell/2$, one at each end of the beam, and N_s stations separated by $N_s - 1$ full fields of length, $\Delta\ell$, where $\Delta\ell = \ell/N_s$ and ℓ is the total length of the beam. The transfer matrix

transfers the displacements (u, w, ψ) and the forces (M, Q, N) from the left side of the field or station to the right side of the same field or station.

Figure 3 shows the flexural configuration of the i^{th} station. From continuity and static equilibrium considerations of Fig. 3, the following conditions are derived:

$$\begin{aligned} u_i^R &= u_i^L & M_i^R &= M_i^L \\ w_i^R &= w_i^L & Q_i^R &= Q_i^L - q \\ \psi_i^R &= \psi_i^L & N_i^R &= N_i^L \end{aligned} \quad (17)$$

The above equations can be written in matrix notation as follows:

$$\begin{bmatrix} u \\ w \\ \psi \\ M \\ Q \\ N \\ 1 \end{bmatrix}_i^R = \begin{bmatrix} 1 & 0 & 0 & 0 & 0 & 0 & 0 \\ 0 & 1 & 0 & 0 & 0 & 0 & 0 \\ 0 & 0 & 1 & 0 & 0 & 0 & 0 \\ 0 & 0 & 0 & 1 & 0 & 0 & 0 \\ 0 & 0 & 0 & 0 & 1 & 0 & -q_s \\ 0 & 0 & 0 & 0 & 0 & 1 & 0 \\ 0 & 0 & 0 & 0 & 0 & 0 & 1 \end{bmatrix} \begin{bmatrix} u \\ w \\ \psi \\ M \\ Q \\ N \\ 1 \end{bmatrix}_i^L \quad (18)$$

Matrix eqn (18) can be written in more compact notation as

$$[S]_i^R = [T_s]_i [S]_i^L \quad (19)$$

where the definitions of each term can be ascertained easily by direct comparison between eqns (18) and (19). The matrix $[T_s]$ is known as the station matrix.

Figure 4 illustrates the flexural configuration for the i^{th} massless

beam element (field). Here, $[S]_i^R$ (station i) = $[S]_i^L$ (field i) and $[S]_i^R$ (field i) = $[S]_{i+1}^L$ (station $i+1$). From equilibrium considerations the following expressions are evident:

$$N_{i+1}^L = N_i^R \quad ; \quad Q_{i+1}^L = Q_i^R - K_q \quad ; \quad M_{i+1}^L = M_i^R + Q_i^R \Delta \ell - K_m \quad (20)$$

where*

$$K_q = \int_0^{\Delta \ell} q(\xi) d\xi \quad ; \quad K_m = \int_0^{\Delta \ell} \xi q(\xi) d\xi \quad (21)$$

Eqns (3) can be inverted to become:

$$\begin{Bmatrix} u, x \\ \psi, x \end{Bmatrix} = \frac{1}{B^2 - AD} \begin{bmatrix} -D & B \\ B & -A \end{bmatrix} \begin{Bmatrix} N \\ M \end{Bmatrix} \quad (22)$$

$$w, x = (Q/S) - \psi$$

From eqn (22), one can write the following equations by taking the averages of the respective moments and axial forces at both ends of the field:

$$u_{i+1}^L = u_i^R + \frac{\Delta \ell}{\gamma} \left[\frac{B(M_{i+1}^L + M_i^R)}{2} - \frac{D(N_{i+1}^L + N_i^R)}{2} \right] \quad (23)$$

$$\psi_{i+1}^L = \psi_i^R - \frac{\Delta \ell}{\gamma} \left[\frac{A(M_{i+1}^L + M_i^R)}{2} - \frac{B(N_{i+1}^L + N_i^R)}{2} \right]$$

where $\gamma \equiv B^2 - AD$.

Making use of eqns (20), one can write equations (23) as:

$$u_{i+1}^L = u_i^R + \left(\frac{B \Delta \ell}{\gamma} \right) M_i^R + \left[\frac{B(\Delta \ell)^2}{\gamma} \right] Q_i^R - \left(\frac{D \Delta \ell}{\gamma} \right) N_i^R - \left(\frac{B \Delta \ell}{2\gamma} \right) K_m \quad (24)$$

$$\psi_{i+1}^L = \psi_i^R - \left(\frac{A \Delta \ell}{\gamma} \right) M_i^R - \left[\frac{A(\Delta \ell)^2}{2\gamma} \right] Q_i^R + \left(\frac{B \Delta \ell}{\gamma} \right) N_i^R + \left(\frac{A \Delta \ell}{2\gamma} \right) K_m$$

Similarly, eqns (22), (20), and (23), can be combined to yield the following:

* Values for K_q and K_m for several different loading conditions are listed in Table 1.

$$w_{i+1}^L = w_i^R + \left[\frac{\Delta\ell}{S} + \frac{A(\Delta\ell)^3}{4\gamma} \right] Q_i^R + \left[\frac{A(\Delta\ell)^2}{2\gamma} \right] M_i^R - \left[\frac{B(\Delta\ell)^2}{2\gamma} \right] N_i^R \\ - (\Delta\ell) \psi_i^R - \left[\frac{A(\Delta\ell)}{2\gamma} \right] K_m + \frac{\Delta\ell}{2S} K_q \quad (25)$$

In matrix notation, eqns (20), (24), and (25) become

$$\begin{bmatrix} u \\ w \\ \psi \\ M \\ Q \\ N \\ 1 \end{bmatrix}_{i+1}^L = \begin{bmatrix} 1 & 0 & 0 & \frac{B\Delta\ell}{\gamma} & \frac{B(\Delta\ell)^2}{2\gamma} & \frac{-B\Delta\ell}{\gamma} & \frac{-B\Delta\ell}{2\gamma} K_m \\ 0 & 0 & -A\Delta\ell & \frac{A(\Delta\ell)^2}{2\gamma} & \left[\frac{\Delta\ell}{S} + \frac{A(\Delta\ell)^3}{4\gamma} \right] & \frac{-B(\Delta\ell)^2}{2\gamma} & \frac{-A(\Delta\ell)^2}{4\gamma} K_m - \frac{\Delta\ell}{2S} K_q \\ 0 & 0 & 1 & \frac{-A\Delta\ell}{\gamma} & \frac{-A(\Delta\ell)^2}{2\gamma} & \frac{B\Delta\ell}{\gamma} & \frac{A\Delta\ell}{2\gamma} K_m \\ 0 & 0 & 0 & 1 & \Delta\ell & 0 & -K_m \\ 0 & 0 & 0 & 0 & 1 & 0 & -K_q \\ 0 & 0 & 0 & 0 & 0 & 1 & 0 \\ 0 & 0 & 0 & 0 & 0 & 0 & 1 \end{bmatrix} \begin{bmatrix} u \\ w \\ \psi \\ M \\ Q \\ N \\ 1 \end{bmatrix}_i^R \quad (26)$$

which can also be written as

$$[S]_{i+1}^L = [T_j] [S]_i^R \quad (27)$$

The matrix $[T_j]$ is known as the field matrix.

The station and field matrices, eqns (19) and (27), can be used to give the relationship of the state vectors at the two ends of the beam by systematically applying the matrices to each station and field as follows:

$$[S]_{N_s+1}^L = [T_j] \Delta\ell/2 [T_s] \prod_{i=1}^{N_s-1} \{ [T_j] \Delta\ell [T_s] \}_i [T_j] \Delta\ell/2 [S]_0 \quad (28)$$

where $\Delta\ell/2$ is the length of each of the half fields at the ends of the beam and $\Delta\ell$ is the length of each of the whole fields. Eqn (28) can be written in compact form as

$$[S]_{N_s+1} = [R][S]_0 \quad (29)$$

Given the boundary conditions, eqn (29) can be solved for the state vectors at the ends, which are $[S]_0$ and $[S]_{N_s+1}$; see Appendix C of [40].

Finally, the rest of the state vectors are calculated as follows:

$$\begin{aligned} [S]_1 &= [T_j]_{\Delta\ell/2} [S]_0 \\ [S]_1^R &= [T_s] [T_j]_{\Delta\ell/2} [S]_0 \\ [S]_2^L &= [T_j]_{\Delta\ell} [T_s] [T_j]_{\Delta\ell/2} [S]_0 \\ &\cdot \\ &\cdot \\ &\cdot \\ &\cdot \\ [S]_{N_s}^R &= [T_s] \cdot \cdot \cdot [T_s] [T_j]_{\Delta\ell/2} [S]_0 \end{aligned} \quad (30)$$

where the superscripts L and R refer to the left and right sides of the station, respectively.

Values of beam stiffnesses A, B, D, S are needed in order to solve the governing equations. However, for bimodulus beams, neutral-surface positions are required for the computation of A, B, D, S. Study of the expression for neutral-surface position in eqn (7) indicates that, except for a few special cases when neutral-surface positions are known constants, the governing equations must be solved before we can compute neutral-surface positions.

Our approach is first to assume a set of neutral-surface positions

along the beam length, then solve the governing equations for displacements u , w , ψ , and the derivatives u_x and ψ_x . With known values of u_x and ψ_x , compute neutral-surface positions using eqn (7). If the assumed and computed set of neutral-surface positions are in close agreement, the problem is solved. Otherwise, assume a different set of neutral-surface positions and repeat the calculations.

NUMERICAL RESULTS

Numerical results were obtained to verify the validity of application of the transfer-matrix technique to bimodulus-beam problems and to study the behavior of beams made of aramid-cord rubber (a bimodulus material). Unless stated to the contrary, the material properties and beam dimensions listed in Table 2 are employed in all of the problems considered, which are summarized in Table 3. Values of the constants used in Table 3 are as follows:

$$M_0 = M_1 = 0.1 \text{ lb-in.} ; F_1 = 1.0 \text{ lb} ; q_0 = q_2 = 0.1 \text{ lb/in.}$$

The transfer-matrix model of the beam includes twenty-five elements, each of length 0.32 in. A value of 5/6 was used for the shear correction coefficient, K^2 . All of the computations were carried out on an IBM 370 Model 158J computer.

Response of an aramid-cord rubber beam subjected to various loadings is investigated in Cases 1 through 8. Bending moment M , shear force Q , axial force N , and the corresponding displacements including axial elongation (contraction) u , transverse deflection w , bending slope ψ , together with neutral-surface positions z_n , are computed. Results are presented in Tables 4 through 11 for Cases 1 through 8, respectively.

The boundary conditions of Cases 1 through 4 are fairly simple. We have been able to develop both closed-form and transfer-matrix solutions for these cases. The good agreement between closed-form and transfer-matrix results can be seen in Tables 5 through 8. For the majority of the results, the error is less than 2%, although for a few result values which are close to zero, the percentage error can go up to 5%. Actually, accuracy of the transfer-matrix results can be improved by increasing the number of elements into which the beam is divided. The number of elements used in this study is twenty-five which is judged sufficient to give reasonably good results. Support of the judgment is shown in Fig. 5.

Behavior of clamped-free bimodulus beams subjected to uniformly distributed and sinusoidally distributed loads is investigated in Cases 1 and 2. Behavior of bimodulus beams which are also subjected to uniformly distributed and sinusoidally distributed loads but with clamped-clamped boundaries is investigated in Cases 3 and 4. The case of simply-supported boundaries and sinusoidal load can also be solved in closed form for a beam. However, this condition is not discussed here because it is a special one-dimensional case of the plate problem investigated in [36]. For all four Cases 1 through 4, the axial force N is zero. Neutral-surface positions z_n are either constant throughout or piecewise constant. Values of z_n for Cases 1, 2, and 3 are -0.2672, 0.2672, and 0.2672 in., respectively. The value of z_n for Case 4 is 0.2672 in. when $0 \leq x < \ell/2$ and is -0.2672 in. when $\ell/2 < x \leq \ell$. Actually, zero axial force always leads to constant or piecewise constant neutral-surface position; this can be shown using eqn (B.3) from Appendix B and setting $N = 0$ and $M \neq 0$:

$$z_n = B/A = \text{constant} \quad (31)$$

Constant or piecewise-constant neutral-surface position greatly reduces the difficulty in development of closed-form solutions for eqns (6), because eqns (6) can then be reduced to a much simpler form, eqns (8).

If a practicing engineer does not have any access to the technique of analyzing bimodulus structural elements as presented here, the simplest thing he would do is to treat the bimodulus beam as an ordinary beam with Young's modulus taken to be the arithmetic average of the tensile and compressive Young's moduli of the bimodulus material. The question of how good is this approach then arises; the answer is presented in Figs. 6 and 7. The distribution of maximum tensile and maximum compressive normal stresses at the outermost layer of the beam subjected to the condition of Cases 1 and 2 are presented for both approaches in Figs. 6 and 7. In a similar fashion, deflections are compared in Fig. 8. As shown in Figs. 6 and 7, the average-modulus approach results in a maximum normal stress which is approximately 10% of the actual maximum stress (resulting from the bimodulus approach) for both Cases 1 and 2. Figure 8 shows that a maximum deflection approximately 10% of the actual deflection (based on the bimodulus approach) also results from the average-modulus approach. In short, design based on the average-modulus approach would likely lead to premature failure of the structural elements. The technique developed in this work therefore would be valuable to design engineers.

To compare the results of both the transfer-matrix analysis and finite-element analysis with the closed-form solution, Figs. 9 and 10 are presented for Case 3. The finite-element results were provided by Dr. J.N. Reddy [41] and were obtained as a special case of a bimodulus plate [42]. There were twenty-two elements along the length of the beam. Even for the exaggerated

scale used in these figures, it was not possible to show a difference between the transfer-matrix (TM) and closed-form (CF) solutions. The finite-element values were generally smaller than the CF and TM values, except for bending moment, for which all three methods agreed very closely. It was not possible to compare the computation times involved, since the results were run on different machines. However, in the past, it has been the general experience that the TM technique is more efficient [43].

Since closed-form solutions are not available for the complicated boundary conditions considered in Cases 5 through 8, only transfer-matrix results are presented for these cases. The effect of concentrated moment, axial force, and transverse force applied at the free boundary on static behavior of a clamped-free bimodulus beam are investigated for two distributions of loading (uniform and sinusoidal) in Cases 5 and 6. The effect of concentrated moments applied at both boundaries on static behavior of a bimodulus beam subjected to the boundary condition of hinged-hinged with axial constraint are investigated for uniformly distributed and sinusoidal loads in Cases 7 and 8. As shown in Tables 8 through 11, the axial forces N induced by the concentrated moment and forces at the boundaries are constant but not zero; and neutral-surface positions z_n vary drastically along the beam length. In fact a look at eqn (B.3) tells us that if axial force N is nonzero, one would expect z_n generally not to be constant. Although for beams made of ordinary (not bimodulus) material, the neutral surface always coincides with the geometric midplane, the neutral surface for a bimodulus beam is not only far different from the midplane but also assumes various shapes depending on the conditions of boundaries and loadings. Shapes of neutral surfaces for Cases 5 through 8 are illustrated in Fig. 11 through 14.

CONCLUDING REMARKS

In this study, the transfer-matrix model of a bimodulus beam was developed based on shear-deformable-beam theory. Transfer-matrix results were compared with and were in close agreement with closed-form solutions developed herein for all four combinations of uniformly distributed and sinusoidally distributed load with clamped-clamped and clamped-free boundary conditions.

Although closed-form solutions are available only for a number of simple boundary conditions, the transfer-matrix model offers a solution method for a wide variety of boundary and loading conditions. Utilizing the model, behavior of a bimodulus beam was investigated by computing and observing deflections and neutral-surface positions under fairly complicated conditions of loading and boundary. It was found that concentrated forces and moments applied at the boundaries have significant influence on neutral-surface positions; more specifically they can cause the neutral-surface positions (thus stiffnesses) to change drastically along the beam length. As illustrations, plots of neutral-surface positions were presented for some of the investigated cases. Numerical results of displacements and stress distributions were also presented.

A distinguishing feature of the model developed in this work is numerical efficiency. It requires much less computer storage than the variational finite-element method. Also, in a comparison to an exact closed-form solution presented here, the transfer-matrix results were more accurate than the variational finite-element results.

Acknowledgments - The research reported here is based on a portion of the first author's thesis submitted in partial fulfillment of the requirements for the M.S. degree in Mechanical Engineering at the University of Oklahoma, 1981. The authors acknowledge the computing time provided by the Merrick Computing Center of the University of Oklahoma, and helpful discussions and finite-element results from Dr. J.N. Reddy, formerly of the University of Oklahoma, presently at Virginia Polytechnic Institute and State University. The second author acknowledges financial support of the Office of Naval Research, Structural Mechanics Program.

REFERENCES

1. B. Saint-Venant, Notes to the 3rd ed. of Navier's *Résumé des Leçons de la résistance des corps solides*, Paris, 175 (1864).
2. C. Bach and R. Baumann, *Elastizität und Festigkeit*, Springer-Verlag, Berlin, 300-308 (1924).
3. S. Timoshenko, *Strength of Materials*, Pt. II: Advanced Theory and Problems, 2nd ed., Van Nostrand, Princeton, NJ, 362-369 (1941).
4. A. Nadai, *Theory of Flow and Fracture of Solids*, Vol. I, 2nd ed., McGraw-Hill, New York, 353-359 (1950).
5. J. Marin, *Mechanical Behavior of Engineering Materials*, Prentice-Hall, Englewood Cliffs, NJ, 86-88 (1962).
6. S.A. Ambartsumyan, The axisymmetric problem of a circular cylindrical shell made of material with different stiffnesses in tension and compression. *Izvestiya Akademii Nauk SSSR, Mekhanika*, no. 4, 77-85 (1965); Engl. trans., National Tech. Information Center Document AD-675312 (1967).
7. A.A. Shlyakhman and V.A. Lepetov, Calculation of hose for bending. 2. Determining the radius of curvature of the longitudinal axis of hose in bending, taking into account the displacement of the neutral surface. *Soviet Rubber Technology* 18(8), 50-54 (Aug. 1959).

8. E.F. Rybicki and M.F. Kanninen, The effect of different behavior in tension than in compression on the mechanical response of polymeric materials. *Deformation and Fracture of High Polymers* (Battelle Institute Science Colloquium, Kronberg, Germany, Sept. 11-16, 1972), Kausch, H.H., Hassell, J.A., and Jaffee, R.I., Eds., Plenum, New York, 417-427 (1973).
9. S.G. Sterling, The flexural behavior of thermoplastic beams. *Plastics and Polymers* 40, 228-235 (1972).
10. A. Simkin and G. Robin, The mechanical testing of bone in bending. *Journal of Biomechanics* 6, 31-39 (1973).
11. J.G. Williams, Different moduli in tension and compression. *Stress Analysis of Polymers*, Longman, London, 124-126 (1973).
12. F. Tabaddor, Analysis for beams made of bi-modulus elastic orthotropic materials. *Fibre Science and Technology* 9, 51-62 (1967).
13. A.G. Goloyan and A.A. Khachatryan, Bending of beams made of material with different moduli in tension and compression (in Russian). *Doklady Akademii Nauk Armyanskoi SSR* 62, 151-157 (1967). See *Applied Mechanics Reviews* 32, Rev. 190 (1979).
14. V.E. Starzhinskii and V.V. Mozharovskii, Determination of the maximum stresses in a cantilever composed of material with deformation anisotropy. *Polymer Mechanics* 12, 400-405 (1967).
15. T.H. Topper, A.N. Sherbourne, and V. Saari, Bending of glass fibre-reinforced plastic (GFRP) plates on elastic supports. Part I: Material characteristics. *Materials and Structures* 11(62), 75-91 (Mar.-Apr. 1978).
16. J.C. Chapman and J. Slatford, The elastic buckling of brittle columns. *Proceedings, Institution of Civil Engineers* 6, 107-125 (1957).
17. F.Y. Yokel and R.D. Dikkers, Strength of load bearing masonry walls. *Journal of the Structural Division, Proceedings, ASCE* 97(ST5), 1592-1609 (1971).
18. E. Tesfaye and T.J. Broome, Non-symmetrical buckling of walls with no tensile strength. Society for Experimental Stress Analysis, Spring Meeting, Silver Spring, MD, May 1976.
19. Z. Rigbi, The buckling of bimodular columns. *Acta Mechanica* 18, 317-332 (1973).
20. Z. Rigbi and S. Idan, Buckling and immediate postbuckling behavior of bimodular columns. *Journal of Structural Mechanics* 6, 145-164 (1978).
21. N. Kamiya, A refined strain energy formulation for bimodulus material and its application to non-linear bending of a beam. *Transactions, Japan Society for Composite Materials* 1, 10-16 (1976).

22. S.G. Paolinelis, S.A. Paipetis, and P.S. Theocaris, Three-point bending at large deflections of beams with different moduli of elasticity in tension and compression. *Journal of Testing and Evaluation* 1, 177-182 (1979).
23. N. Kamiya, Transverse shear effect in a bimodulus plate. *Nuclear Engineering and Design* 32, 351-357 (1975).
24. R.R. Nachlinger and J.R. Leininger, Bending of a beam made of a fiber-reinforced viscoelastic material. *AIAA Journal* 7, 2016-2017 (1969).
25. A. Vierling and K. Scheele, Die Biegebeanspruchung von Gummi-Fördergurt mit Gewebe-Einlagen. *Kautschuk und Gummi* 14, WT9-WT17 (1961).
26. G.V. Bilida, Mechanical characteristics of oriented glass fiber reinforced plastic loaded in flexure. *Soviet Applied Mechanics* 5, 1211-1214 (1969).
27. N. Phan-Thien, Fibrous materials at non-dilute concentration: interpretation of bending tests. *Fibre Science and Technology* 14, 191-200 (1981).
28. L. Carlsson, C. Fellers, and A. DeRuvo, The mechanism of failure in bending of paperboard. *Journal of Materials Science* 15, 2636-2642 (1980).
29. D.G. Swift and R.S.L. Smith, The flexural strength of cement-based composites using low modulus (sisal) fibres. *Composites* 10, 145-148 (1979).
30. I.M. Kotlyarskii and I.M. Karbasova, Determining the forces occurring in the cross-section of a conveyor belt when it is being bent around a drum. *Soviet Rubber Technology* 27(3), 38-40 (Mar. 1968).
31. R.F. Crawford, An evaluation of boron-polymer film layer composites for high-performance structures. *NASA CR-1114* (Sept. 1968).
32. R.M. Jones and H.S. Morgan, Bending and extension of cross-ply laminates with different moduli in tension and compression. *Computers and Structures* 11, 181-190 (1980).
33. R.M. Jones, Apparent flexural modulus and strength of multi-modulus materials. *Journal of Composite Materials* 10, 342-354 (1976).
34. P.C. Yang, C.H. Norris, and Y. Stavsky, Elastic wave propagation in heterogeneous plates. *International Journal of Solids and Structures* 2, 665-684 (1966).
35. J.M. Whitney and N.J. Pagano, Shear deformation in heterogeneous anisotropic plates. *Journal of Applied Mechanics* 37, 1031-1036 (1970).
36. C.W. Bert, J.N. Reddy, V.S. Reddy, and W.C. Chao, Bending of thick rectangular plates laminated of bimodulus composite materials. *AIAA Journal*, to be published.

37. Y.R. Kan and Y.M. Ito, Shear deformation in heterogeneous anisotropic plates. *Journal of Composite Materials* 6, 316-319 (1972).
38. E.C. Pestel and F.A. Leckie, *Matrix Methods in Elastomechanics*. Van Nostrand, New York, 51-94 (1963).
39. L. Meirovitch, *Analytical Methods in Vibrations*. MacMillan, New York, 251-262 (1967).
40. A.D. Tran, Static and dynamic behavior of bimodulus beams. M.S. thesis, Mechanical Engineering, University of Oklahoma (1981).
41. J.N. Reddy, Private communication. Department of Engineering Science and Mechanics, Virginia Polytechnic Institute and State University, Blacksburg, VA (1981).
42. J.N. Reddy and W.C. Chao, Finite-element analysis of laminated bimodulus plates. *Computers and Structures* 12, 245-251 (1980).
43. C. Chiatti and A. Sestieri, Analysis of static and dynamic structural problems by combined finite element-transfer matrix method. *Journal of Sound and Vibration* 67(1), 35-42 (1979).

APPENDIX A. EFFECT OF NEUTRAL-SURFACE LOCATION ON THE BEAM STIFFNESSES

It is mathematically convenient in the solution of eqns (6) to reduce these equations to an algebraic form not including the integral forms of the A, B, D, and S. Therefore, the expansion of these terms into their form in terms of the two Young's moduli E^k and two shear rigidities G^k is completed in the following manner.

Refer to Fig. A.1 for a typical stress distribution for the case of the neutral-surface location greater than zero; where z_n , the neutral-surface location, is measured positively downward from the geometric midplane. The top of the beam is considered to be $-h/2$ and the bottom of the beam is $h/2$. The beam stiffnesses are defined as follows:

$$A \equiv \int_{-h/2}^{h/2} E^k dz, \quad B \equiv \int_{-h/2}^{h/2} E^k z dz$$

$$D \equiv \int_{-h/2}^{h/2} E^k z^2 dz, \quad S \equiv \int_{-h/2}^{h/2} G^k dz \quad (A.1)$$

where E^k and G^k are the Young's moduli and shear moduli respectively.

Superscript k can be either t or c, which represent tension or compression properties respectively.

Convex Downward Bending

In convex downward bending, the top layer of a beam is in compression and the bottom layer in tension.

The first of eqns (A.1) can be expanded in the following form:

$$A = \int_{-h/2}^{z_n} E^c dz + \int_{z_n}^{h/2} E^t dz = [z_n + (h/2)]E^c + [(h/2) - z_n]E^t$$

or

$$A = (h/2)(E^c + E^t) + (E^c - E^t)z_n \quad (A.2)$$

In similar form, the second of eqns (A.1) can be expanded to:

$$B = \int_{-h/2}^{z_n} E^c z dz + \int_{z_n}^{h/2} E^t z dz = \frac{E^c}{2} (z_n^2 - \frac{h^2}{4}) + \frac{E^t}{2} (\frac{h^2}{4} - z_n^2)$$

or

$$B = - (h^2/8)(E^c - E^t) + (1/2)(E^c - E^t)z_n^2 \quad (A.3)$$

Also

$$D = \int_{-h/2}^{z_n} E^c z^2 dz + \int_{z_n}^{h/2} E^t z^2 dz = (1/3)(z_n^2 + \frac{h^3}{8})E^c + (1/3)(\frac{h^3}{8} - z_n^3)E^t$$

or

$$D = (h^3/24)(E^c + E^t) + (1/3)(E^c - E^t)z_n^3 \quad (A.4)$$

and

$$S = \int_{-h/2}^{z_n} G^c dz + \int_{z_n}^{h/2} G^t dz = [z_n + (h/2)]G^c + [(h/2) - z_n]G^t$$

or

$$S = (h/2)(G^c + G^t) + (G^c - G^t)z_n \quad (A.5)$$

Concave Downward Bending

In concave downward bending, the top layer of beam is in tension and the bottom layer in compression.

The first of eqns (A.1) can be expanded in the following form:

$$A = \int_{-h/2}^{z_n} E^t dz + \int_{z_n}^{h/2} E^c dz = E^t[z_n + (h/2)] + E^c[(h/2) - z_n]$$

or

$$A = (h/2)(E^c + E^t) - z_n(E^c - E^t) \quad (A.6)$$

With a similar approach, the second of eqns (A.1) can be expanded to:

$$B = \int_{-h/2}^{z_n} E^t z dz + \int_{z_n}^{h/2} E^c z dz = \frac{E^t}{2} (z_n^2 - \frac{h^2}{4}) + \frac{E^c}{2} (\frac{h^2}{4} - z_n^2)$$

or

$$B = (h^2/8)(E^c - E^t) - (1/2)(E^c - E^t)z_n^2 \quad (A.7)$$

Also

$$D = \int_{-h/2}^{z_n} E^t z^2 dz + \int_{z_n}^{h/2} E^c z^2 dz = \frac{E^t}{3} (z_n^3 + \frac{h^3}{8}) + \frac{E^c}{3} (\frac{h^3}{8} - z_n^3)$$

or

$$D = (h^3/24)(E^c + E^t) - (1/3)(E^c - E^t)z_n^3 \quad (A.8)$$

and

$$S = \int_{-h/2}^{z_n} G^t dz + \int_{z_n}^{h/2} G^c dz = G^t(z_n + \frac{h}{2}) + G^c(\frac{h}{2} - z_n)$$

or

$$S = (h/2)(G^c + G^t) - (G^c - G^t)z_n \quad (A.9)$$

APPENDIX B. METHOD OF COMPUTING NEUTRAL-SURFACE LOCATION FROM MOMENT
DIAGRAM AND AXIAL FORCE

Under certain combinations of loading and boundary conditions, the neutral-surface location varies drastically along the beam length (x-axis). Closed-form solutions currently exist only for cases in which the neutral-surface location is constant along the beam length. However, the transfer-matrix technique can be utilized to analyze cases of varying neutral-surface location. Evidently some benchmark is needed to verify the latter technique's application to bimodulus problems. It is a fairly simple task to derive the moment diagram from boundary conditions and applied axial force. Results of this method have then been checked against those of transfer-matrix analysis; good agreement was obtained.

The constitutive relation for a bimodulus beam with provision for a shift of neutral-surface location (due to different properties in tension and compression) has been written in eqn (22) as follows:

$$\begin{Bmatrix} u_x^0 \\ \psi_x \end{Bmatrix} = \frac{1}{B^2 - AD} \begin{bmatrix} -D & B \\ B & -A \end{bmatrix} \begin{Bmatrix} N \\ M \end{Bmatrix} \quad (B.1)$$

From the kinematics of deformation, the neutral-surface location has been derived and expressed in eqn (7) as follows:

$$z_n = -u_x^0 / \psi_x \quad (B.2)$$

Replacing u_x^0 and ψ_x by the expressions in eqn (B.1), one can rewrite eqn (B.2) as

$$z_n = (BM - DN) / (AM - BN) \quad (B.3)$$

Study of eqns (A.2) - (A.4) and (A.6) - (A.8) indicates that the expressions for stiffnesses A, B, D can be written as

$$A = a_1 + a_2 z_n \quad ; \quad B = b_1 + b_2 z_n^2 \quad ; \quad D = d_1 + d_2 z_n^3 \quad (B.4)$$

where for concave bending

$$\begin{aligned} a_1 &= (h/2)(E^c + E^t) \quad ; \quad a_2 = E^c - E^t \\ b_1 &= -(h^2/8)(E^c - E^t) \quad ; \quad b_2 = (1/2)(E^c - E^t) \\ d_1 &= (h^3/24)(E^c + E^t) \quad ; \quad d_2 = (1/3)(E^c - E^t) \end{aligned} \quad (B.5.a)$$

and for convex bending

$$\begin{aligned} a_1 &= (h/2)(E^c + E^t) \quad ; \quad a_2 = -(E^c - E^t) \\ b_1 &= (h^2/8)(E^c - E^t) \quad ; \quad b_2 = -(1/2)(E^c - E^t) \\ d_1 &= (h^3/24)(E^c + E^t) \quad ; \quad d_2 = -(1/3)(E^c - E^t) \end{aligned} \quad (B.5.b)$$

Replacing stiffnesses A, B, D by the expression in eqns (B.4), one can write eqn (B.3) as

$$M[z_n^2(a_2 - b_2) + a_1 z_n - b_1] = [z_n^3(b_2 - d_2) + b_1 z_n - d_1]N \quad (B.6)$$

Once moment M and axial force N are known, eqn (B.6) can be solved for z_n .

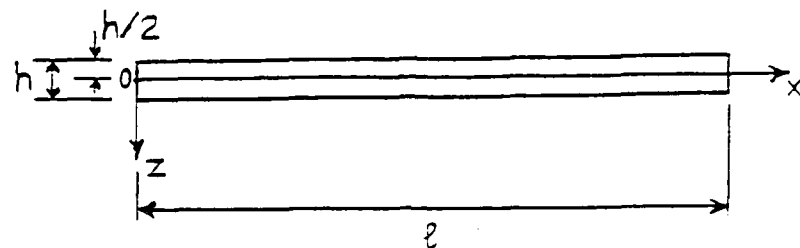


Fig. 1 Cartesian coordinate system for beam.

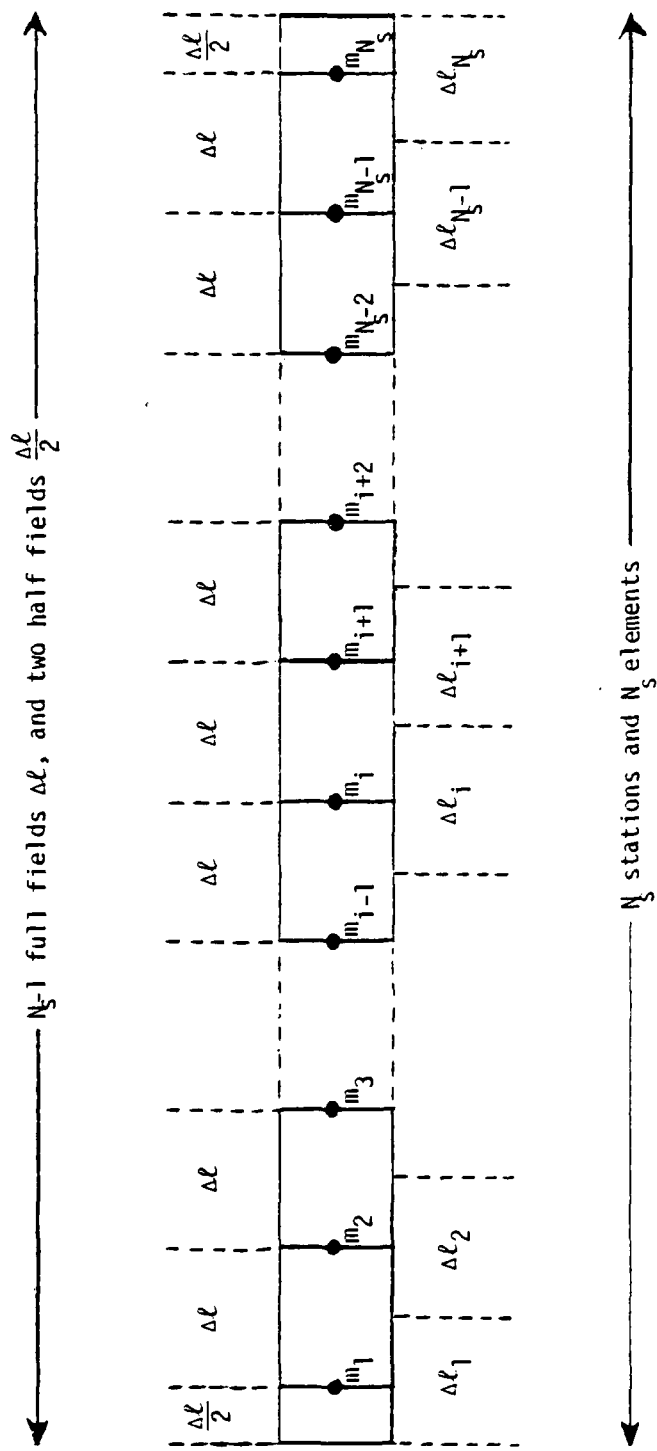


Fig. 2 Field and station model of a beam.

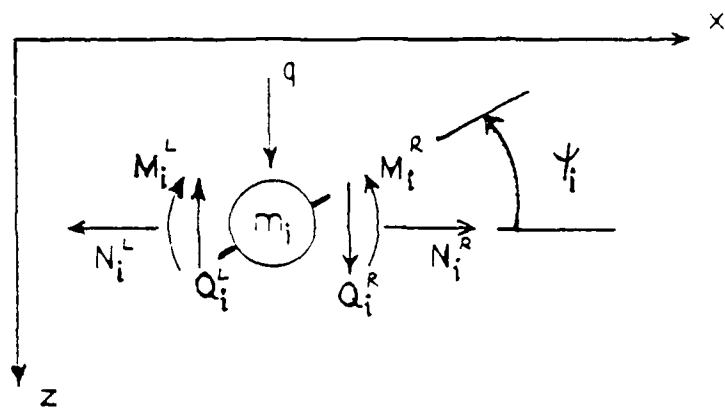


Fig. 3 Flexural configuration of i^{th} station.

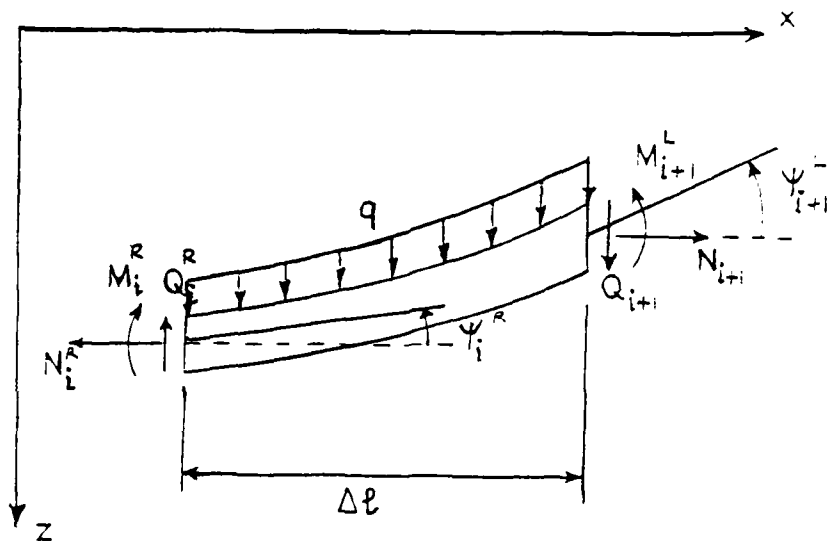


Fig. 4 Flexural configuration of i^{th} field.

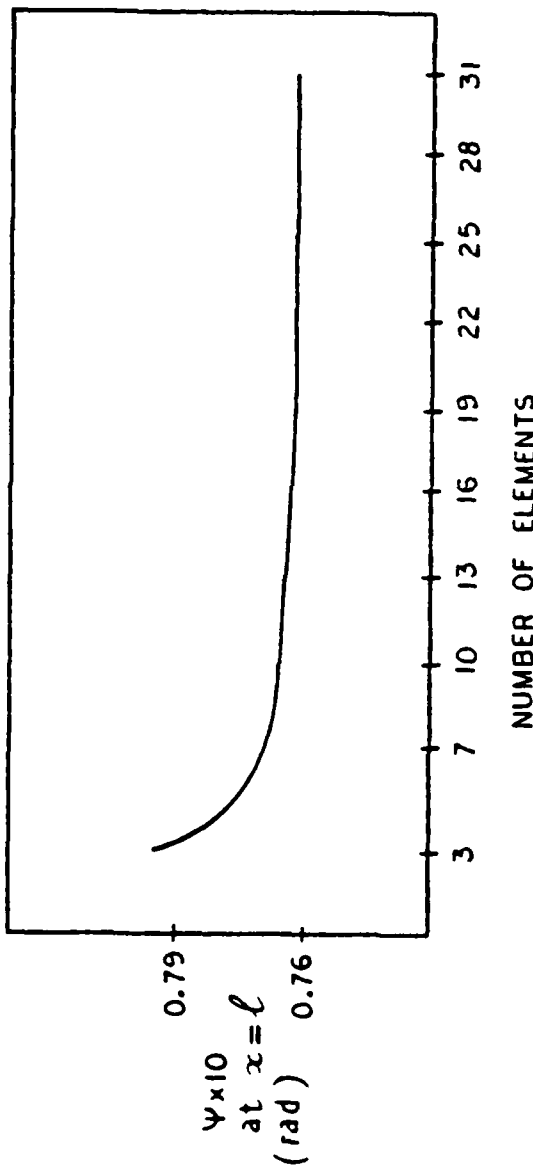


Fig. 5 Effect of number of beam elements on numerical value for bending slope (at $x = l$) of an aramid-cord rubber beam (Case 1).

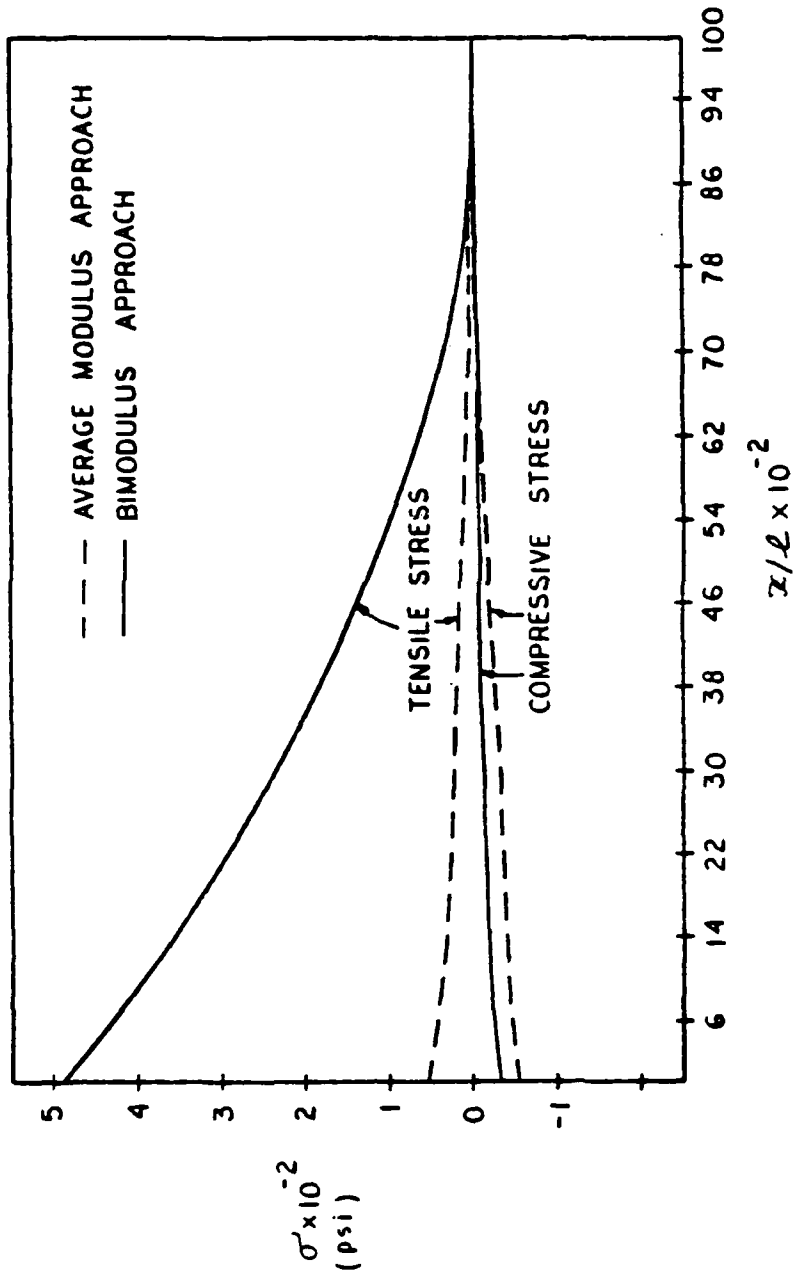


Fig. 6. Comparison between the maximum tensile and compressive normal stress distributions of an aramid-cord rubber beam and an ordinary beam having a Young's modulus which is the arithmetic average of tensile and compressive Young's moduli of aramid-cord rubber (Case 1).

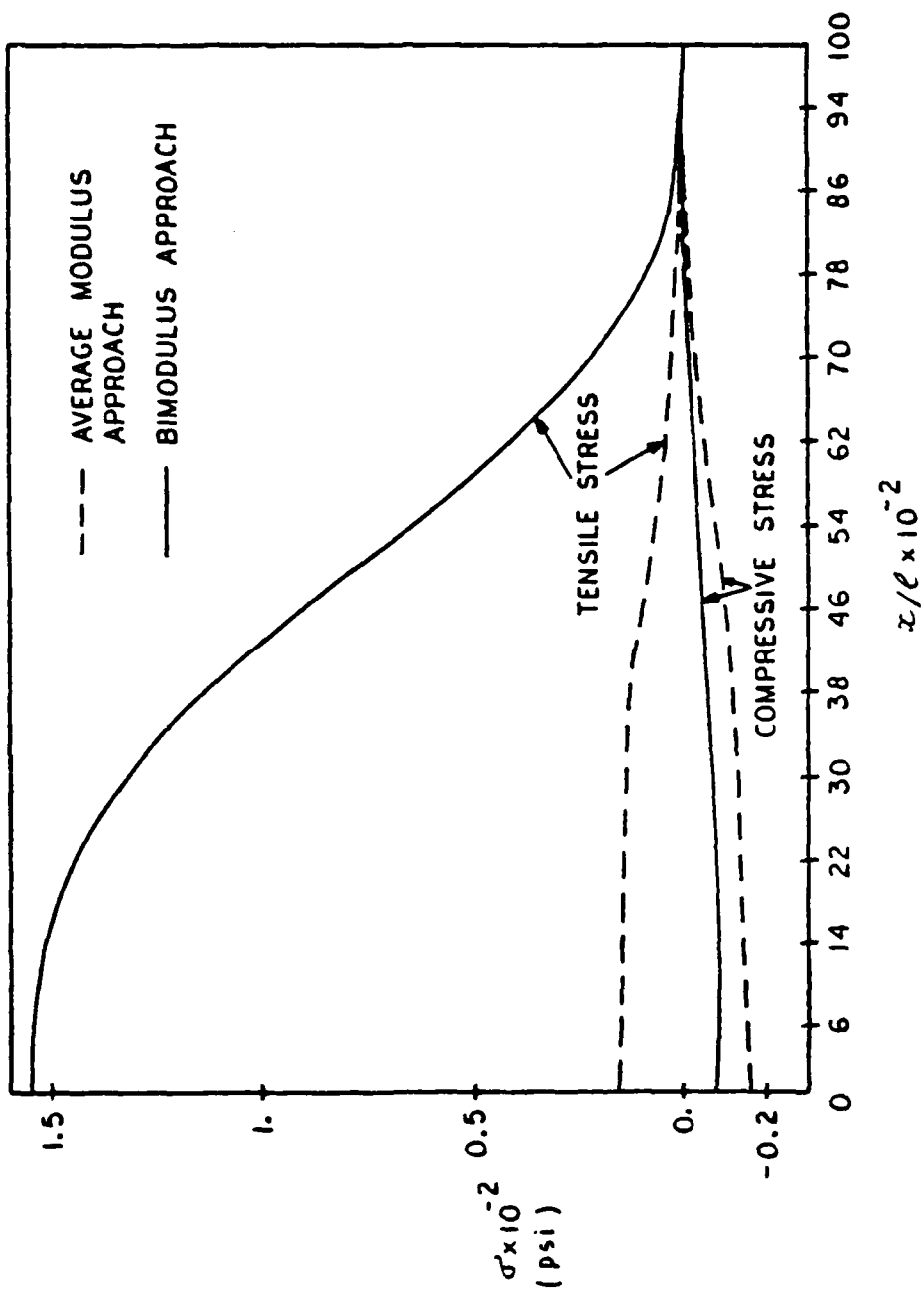


Fig. 7. Comparison between the maximum tensile and compressive normal stress distributions of an aramid-cord rubber beam and an ordinary beam having Young's modulus which is the arithmetic average of tensile and compressive Young's moduli of aramid-cord rubber (Case 2).

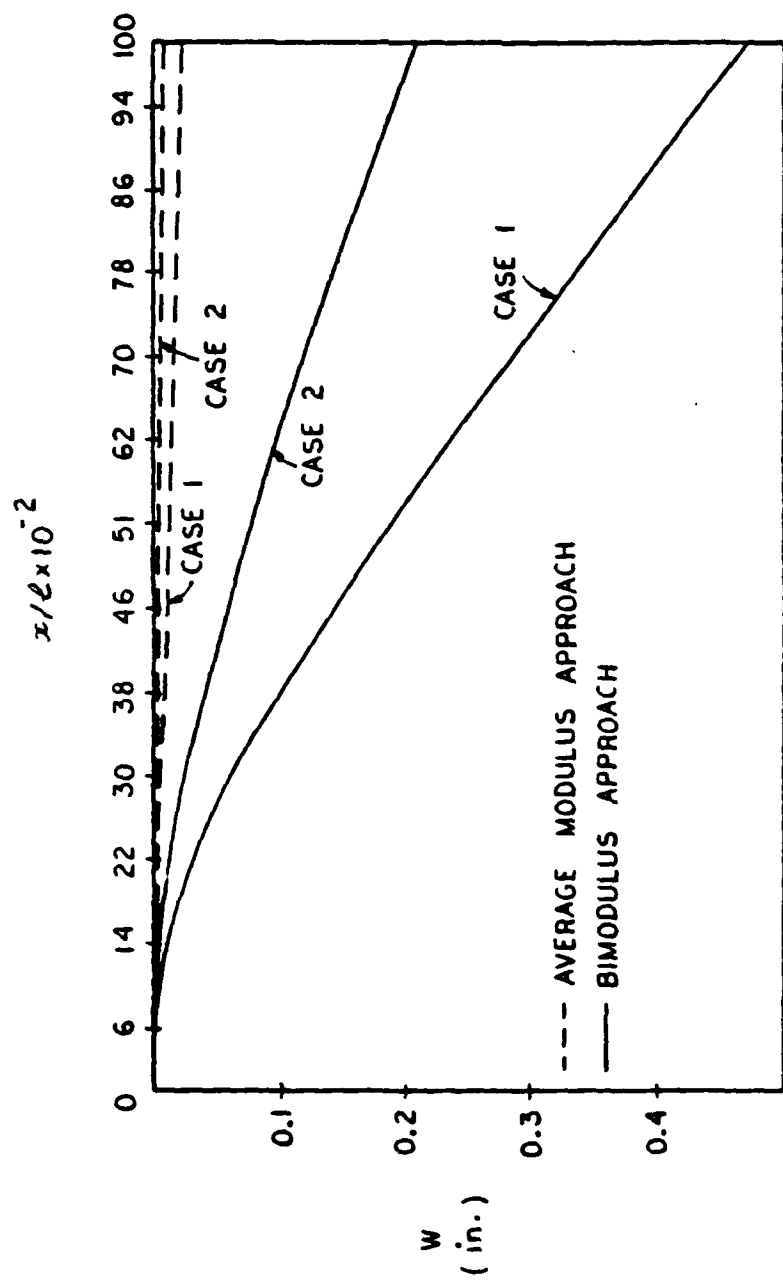


Fig. 8. Comparison between deflection distribution of an aramid-cord rubber beam and an ordinary beam having a Young's modulus which is equal to the arithmetic average of tensile and compressive Young's moduli of aramid-cord rubber (Cases 1 and 2).

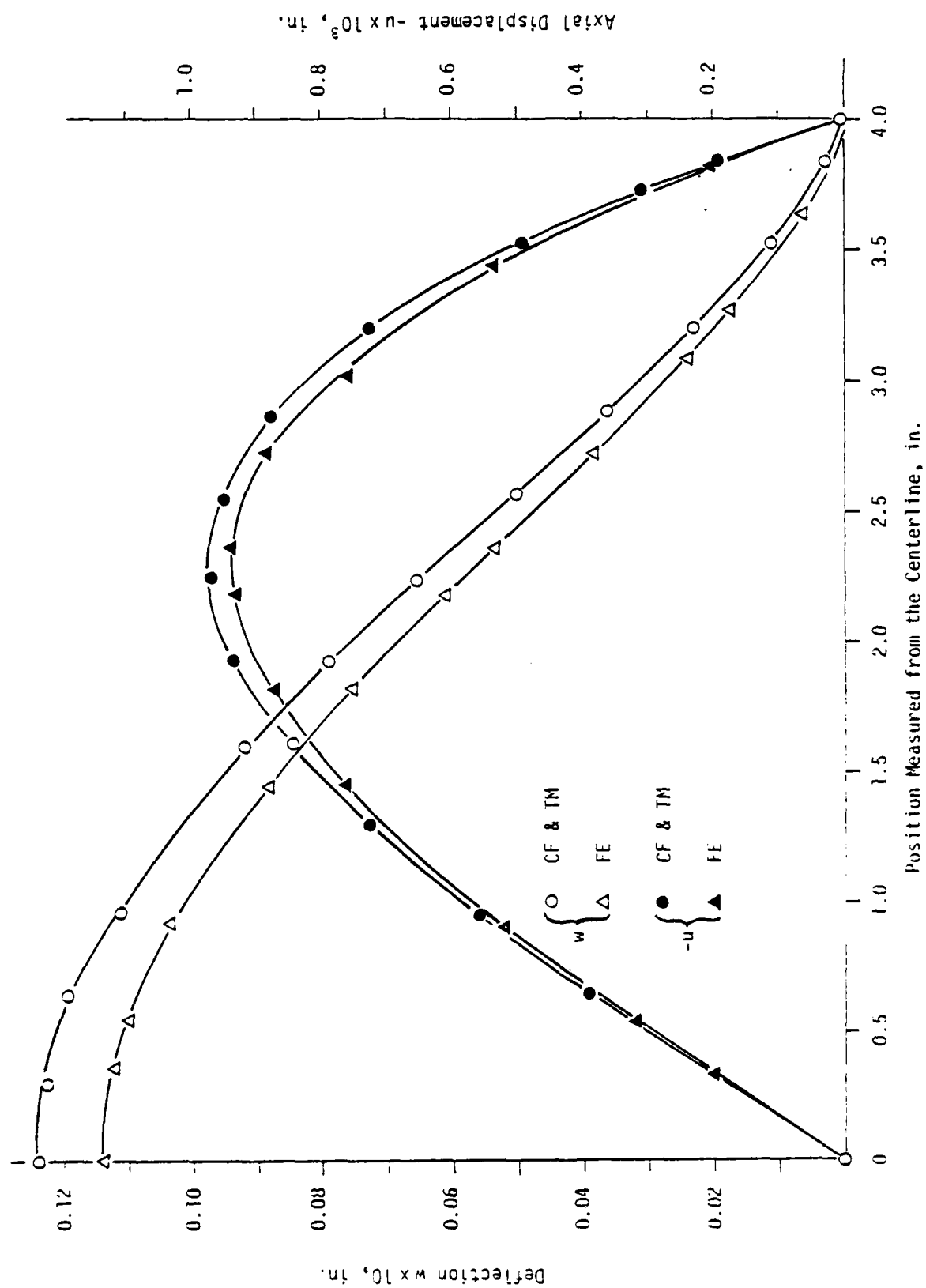


Fig. 9. Deflection and axial displacement for Case 3 as calculated by three different methods: closed form (CF), finite element (FE), and transfer matrix (TM).

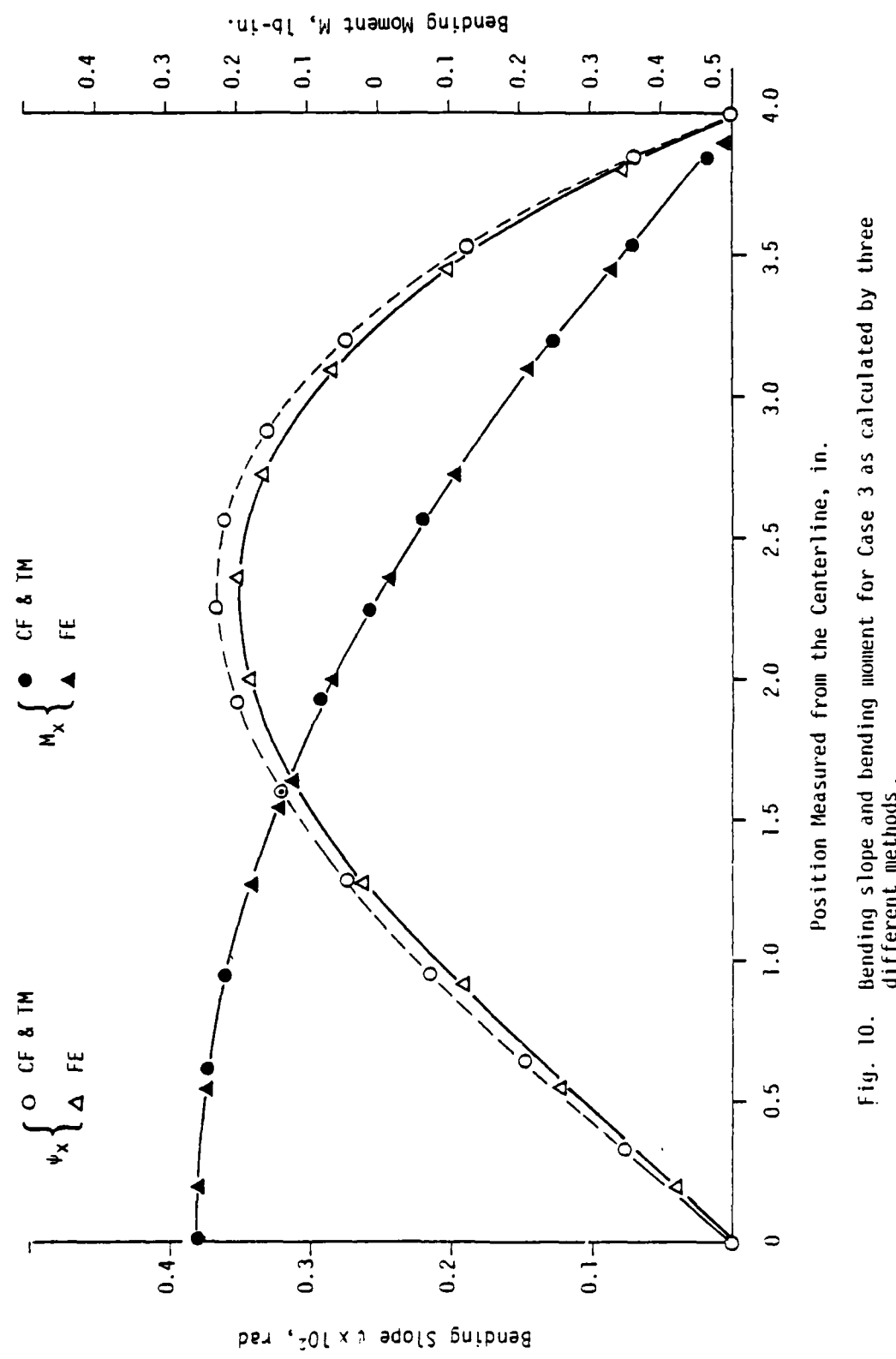


Fig. 10. Bending slope and bending moment for Case 3 as calculated by three different methods.

 REGION IN COMPRESSION

 REGION IN TENSION



Fig. 11. Neutral-surface shape of an aramid-cord rubber beam (Case 5).



Fig. 12. Neutral-surface shape of an aramid-cord rubber beam (Case 6).



Fig. 13. Neutral-surface shape of an aramid-cord rubber beam (Case 7).

 REGION IN COMPRESSION

 REGION IN TENSION

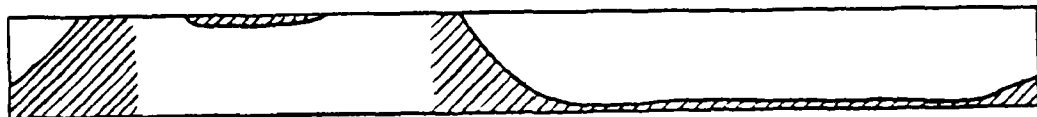


Fig. 14. Neutral-surface shape of an aramid-cord rubber beam (Case 8).

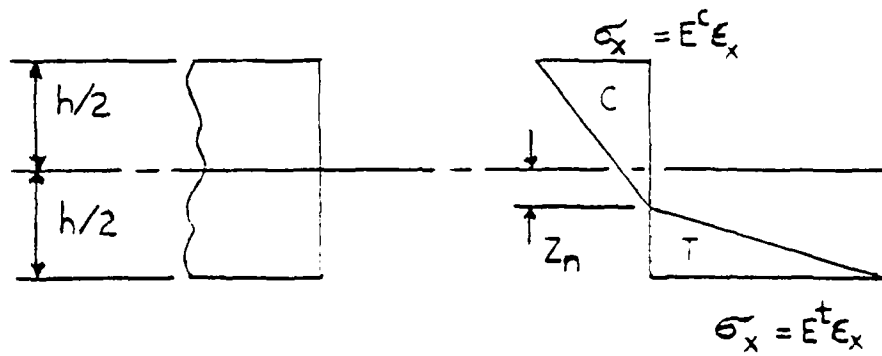


Fig. A-1 Typical stress distribution for a bimodulus beam with neutral-surface position greater than zero.

Table 1. Values of K_m and K_q for various loading conditions

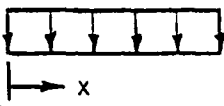
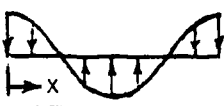
Loading condition (on the whole beam)	K_m	K_q
Uniform load $q(x) = q_0$ 	$q_0(\Delta\ell)^2/2$	$q_0\Delta\ell$
Sine load $q(x) = q_0 \sin \frac{n\pi}{\ell} x$ 	$\frac{q_0\ell}{n\pi} [\ell \cos \frac{n\pi}{\ell} x_{j-1} - \frac{\ell}{n\pi} (\sin \frac{n\pi}{\ell} x_j - \sin \frac{n\pi}{\ell} x_{j-1})]$	$-\frac{q_0\ell}{n\pi} (\cos \frac{n\pi}{\ell} x_j - \cos \frac{n\pi}{\ell} x_{j-1})$
Cosine load $q(x) = q_0 \cos \frac{n\pi}{\ell} x$ 	$\frac{q_0\ell}{n\pi} [-\frac{\ell}{n\pi} (\cos \frac{n\pi}{\ell} x_j - \cos \frac{n\pi}{\ell} x_{j-1}) - \ell \sin \frac{n\pi}{\ell} x_{j-1}]$	$\frac{q_0\ell}{n\pi} (\sin \frac{n\pi}{\ell} x_j - \sin \frac{n\pi}{\ell} x_{j-1})$

Table 2. Pertinent elastic and physical properties [36] and geometric parameters for aramid-cord rubber beam

Properties and Units	Tension	Compression
Longitudinal Young's modulus, psi	5.193×10^5	1.740×10^3
Longitudinal-thickness shear modulus, psi	5.366×10^2	5.366×10^2
Density, lbf/in^3	0.037	0.037
Beam length	8 in.	
Beam depth (thickness)	0.6 in.	

Table 3. Summary of all problem cases considered

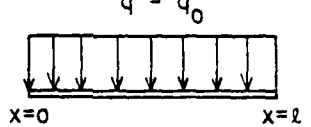
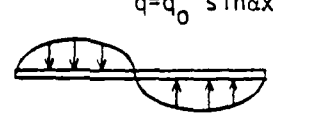
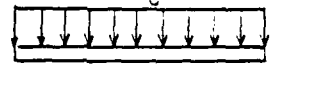
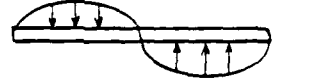
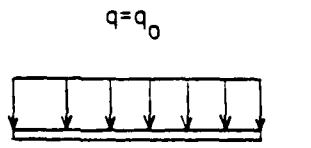
Case No.	Boundary conditions	Spatial distribution of distributed load	Time variation of distributed load
1	CLAMPED-FREE	$q = q_0$  UNIFORMLY DISTRIBUTED	STATIC
2	CLAMPED-FREE	$q = q_0 \sin \alpha x$  $x=0 \quad x=l$ SINUSOIDAL ($\alpha = 2\pi/l$)	STATIC
3	CLAMPED-CLAMPED WITH AXIAL CONSTRAINT	$q = q_0$  $x=0 \quad x=l$ UNIFORMLY DISTRIBUTED	STATIC
4	CLAMPED-CLAMPED WITH AXIAL CONSTRAINT	$q = q_0 \sin \alpha x$  $x=0 \quad x=l$ SINUSOIDAL ($\alpha = 2\pi/l$)	STATIC
5	CLAMPED-FREE WITH MOMENT AND FORCES APPLIED AT THE FREE END	$q = q_0$  $x=0 \quad x=l$ UNIFORMLY DISTRIBUTED	STATIC

Table 3. (continued)

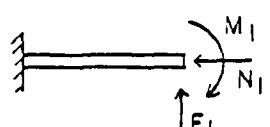
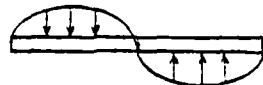
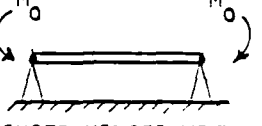
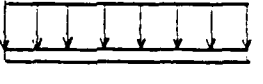
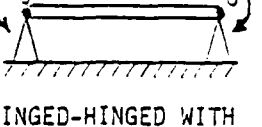
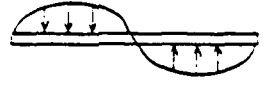
Case No.	Boundary conditions	Spatial distribution of distributed load	Time variation of distributed load
6	 CLAMPED-FREE WITH MOMENT AND FORCES APPLIED AT THE FREE END	$q = q_0 \sin \alpha x$  $x=0$ SINUSOIDAL ($\alpha=2\pi/l$)	STATIC
7	 HINGED-HINGED WITH MOMENTS APPLIED AT BOTH ENDS AND AXIAL CONSTRAINT	$q = q_0$  $x=0$ $x=l$ UNIFORMLY DISTRIBUTED	STATIC
8	 HINGED-HINGED WITH MOMENTS APPLIED AT BOTH ENDS AND AXIAL CONSTRAINT	$q = q_0 \sin \alpha x$  $x=0$ SINUSOIDAL ($\alpha=2\pi/l$)	STATIC

Table 4. Comparison between closed-form and transfer-matrix solutions for an aramid-cord rubber beam (Case 1)

x/l	u x 10 ³ in		w ₂ in		ψ x 10 ³ rad		M. lb-in		q, lb	
	CF*	TM*	CF*	TM*	CF*	TM*	CF*	TM*	CF*	TM*
0.00	0.0000	0.0000	0.0000	0.0000	0.0000	0.0000	-3.2000	-3.2000	0.8000	0.8000
0.02	-0.0119	-0.0119	0.0008	0.0008	-0.0448	-0.0448	-3.0730	-3.0730	0.7840	0.7840
0.06	-0.0345	-0.0345	0.0045	0.0045	-0.1292	-0.1291	-2.8280	-2.8280	0.7520	0.7520
0.10	-0.0551	-0.0551	0.0108	0.0107	-0.2065	-0.2066	-2.5920	-2.5920	0.7200	0.7200
0.14	-0.0741	-0.0741	0.0194	0.0193	-0.2773	-0.2774	-2.3670	-2.3670	0.6880	0.6880
0.18	-0.0913	-0.0913	0.0301	0.0300	-0.3419	-0.3420	-2.1520	-2.1520	0.6560	0.6560
0.22	-0.1070	-0.1070	0.0428	0.0427	-0.4004	-0.4005	-1.9470	-1.9470	0.6240	0.6240
0.26	-0.1211	-0.1211	0.0571	0.0571	-0.4533	-0.4534	-1.7520	-1.7520	0.6920	0.6920
0.30	-0.1338	-0.1338	0.0731	0.0730	-0.5007	-0.5008	-1.5680	-1.5680	0.5600	0.5600
0.34	-0.1451	-0.1451	0.0905	0.0904	-0.5430	-0.5432	-1.3940	-1.3940	0.5280	0.5280
0.38	-0.1551	-0.1551	0.1091	0.1090	-0.5804	-0.5807	-1.2300	-1.2300	0.4960	0.4960
0.42	-0.1639	-0.1639	0.1288	0.1287	-0.6134	-0.6136	-1.0760	-1.0760	0.4640	0.4640
0.46	-0.1715	-0.1716	0.1494	0.1493	-0.6421	-0.6423	-0.9331	-0.9331	0.4320	0.4320
0.50	-0.1781	-0.1782	0.1709	0.1708	-0.6668	-0.6671	-0.8000	-0.8000	0.4000	0.4000
0.54	-0.1838	-0.1839	0.1930	0.1929	-0.6879	-0.6882	-0.6771	-0.6771	0.3680	0.3680
0.58	-0.1885	-0.1886	0.2157	0.2156	-0.7056	-0.7059	-0.5645	-0.5645	0.3360	0.3360
0.62	-0.1924	-0.1925	0.2390	0.2388	-0.7202	-0.7206	-0.4621	-0.4621	0.3040	0.3040
0.66	-0.1956	-0.1957	0.2625	0.2625	-0.7321	-0.7325	-0.3699	-0.3699	0.2720	0.2720
0.70	-0.1981	-0.1982	0.2864	0.2863	-0.7415	-0.7419	-0.2880	-0.2880	0.2400	0.2400
0.74	-0.2000	-0.2001	0.3105	0.3105	-0.7487	-0.7491	-0.2163	-0.2163	0.2080	0.2080
0.78	-0.2014	-0.2015	0.3348	0.3347	-0.7539	-0.7544	-0.1549	-0.1549	0.1760	0.1760
0.82	-0.2024	-0.2025	0.3592	0.3591	-0.7576	-0.7581	-0.1037	-0.1037	0.1440	0.1440
0.86	-0.2030	-0.2032	0.3836	0.3836	-0.7600	-0.7605	-0.0627	-0.0627	0.1120	0.1120
0.90	-0.2034	-0.2035	0.4081	0.4080	-0.7613	-0.7618	-0.0320	-0.0320	0.0800	0.0800
0.94	-0.2035	-0.2037	0.4325	0.4325	-0.7619	-0.7625	-0.0115	-0.0115	0.0480	0.0480
0.98	-0.2036	-0.2037	0.4570	0.4570	-0.7620	-0.7626	-0.0012	-0.0012	0.0159	0.0159
1.00	-0.2036	-0.2038	0.4692	0.4692	-0.7621	-0.7626	0.0000	0.0000	0.0000	0.0000

* CF denotes closed-form solutions; TM signifies transfer-matrix solution.

Table 5. Comparison between closed-form and transfer-matrix solutions for an aramid-cord rubber beam (Case 2)

x/ℓ	$u \times 10^2$, in		w , in		$\psi \times 10$, rad		M , lb-in		q , lb	
	CF*	TM*	CF*	TM*	CF*	TM*	CF*	TM*	CF*	TM*
0.00	0.0000	0.0000	0.0000	-0.0000	0.0000	0.0000	1.0190	1.0190	0.0000	-0.0000
0.02	-0.0388	-0.0388	-0.0001	-0.0001	0.0145	0.0145	1.0190	1.0190	-0.0010	-0.0010
0.06	-0.1166	-0.1166	-0.0010	-0.0010	0.0436	0.0436	1.0170	1.0170	-1.0089	-0.0089
0.10	-0.1941	-0.1941	-0.0029	-0.0029	0.0726	0.0726	1.0120	1.0120	-0.0243	-0.0243
0.14	-0.2710	-0.2709	-0.0057	-0.0057	0.1014	0.1014	1.0010	1.0010	-0.0461	-0.0461
0.18	-0.3467	-0.3466	-0.0095	-0.0095	0.1298	0.1297	0.9819	0.9819	-0.0731	-0.0731
0.22	-0.4207	-0.4205	-0.0142	-0.0142	0.1575	0.1574	0.9537	0.9537	-0.1035	-0.1035
0.26	-0.4921	-0.4918	-0.0198	-0.0198	0.1842	0.1841	0.9155	0.9155	-0.1353	-0.1353
0.30	-0.5602	-0.5599	-0.0263	-0.0263	0.2097	0.2096	0.8672	0.8672	-0.1667	-0.1667
0.34	-0.6243	-0.6239	-0.0336	-0.0336	0.2337	0.2335	0.8091	0.8091	-0.1955	-0.1955
0.38	-0.6836	-0.6831	-0.0417	-0.0416	0.2559	0.2557	0.7425	0.7425	-0.2201	-0.2201
0.42	-0.7375	-0.7370	-0.0505	-0.0504	0.2760	0.2759	0.6689	0.6689	-0.2389	-0.2389
0.46	-0.7856	-0.7851	-0.0599	-0.0598	0.2940	0.2939	0.5903	0.5903	-0.2506	-0.2506
0.50	-0.8274	-0.8269	-0.0698	-0.0698	0.3097	0.3095	0.5095	0.5095	-0.2546	-0.2546
0.54	-0.8633	-0.8628	-0.0803	-0.0802	0.3232	0.3230	0.4282	0.4282	-0.2506	-0.2506
0.58	-0.8930	-0.8925	-0.0911	-0.0910	0.3343	0.3341	0.3497	0.3497	-0.2389	-0.2389
0.62	-0.9169	-0.9164	-0.1023	-0.1022	0.3432	0.3430	0.2761	0.2761	-0.2201	-0.2201
0.66	-0.9353	-0.9349	-0.1136	-0.1135	0.3501	0.3500	0.2094	0.2094	-0.1955	-0.1955
0.70	-0.9491	-0.9487	-0.1251	-0.1250	0.3552	0.3551	0.1514	0.1514	-0.1667	-0.1667
0.74	-0.9587	-0.9584	-0.1367	-0.1366	0.3588	0.3587	0.1030	0.1030	-0.1353	-0.1353
0.78	-0.9651	-0.9648	-0.1484	-0.1483	0.3612	0.3611	0.0648	0.0648	-0.1035	-0.1035
0.82	-0.9689	-0.9687	-0.1601	-0.1599	0.3627	0.3626	0.0366	0.0366	-0.0731	-0.0731
0.86	-0.9709	-0.9708	-0.1718	-0.1716	0.3634	0.3634	0.0176	0.0176	-0.0461	-0.0461
0.90	-0.9718	-0.9717	-0.1835	-0.1833	0.3637	0.3637	0.006561	0.006561	-0.0243	-0.0243
0.94	-0.9720	-0.9720	-0.1951	-0.1950	0.3638	0.3638	0.001426	0.001426	-0.0089	-0.0089
0.96	-0.9721	-0.9721	-0.2068	-0.2066	0.3639	0.3639	0.00004	0.00004	-0.0010	-0.0010
1.00	-0.9721	-0.9721	-0.2126	-0.2124	0.3639	0.3639	0.0000	0.0000	0.0000	0.0000

* CF denotes closed-form solutions; TM signifies transfer-matrix solution.

Table 6. Comparison between closed-form and transfer-matrix solutions for an aramid-cord rubber beam (Case 3)

x/t	$u \times 10^3$, in		$w_x \times 10^2$, in		$\psi_x \times 10^2$, rad		M_x , lb-in		q , lb	
	CF*	TM*	CF*	TM*	CF*	TM*	CF*	TM*	CF*	TM*
0.00	0.0000	0.0000	0.0000	0.0000	0.0000	0.0000	-0.5333	-0.5325	0.4000	0.4000
0.02	0.1913	0.1913	0.0292	0.0291	-0.0716	-0.0716	-0.4706	-0.4698	0.3840	0.3840
0.06	0.5052	0.5050	0.1157	0.1147	-0.1891	-0.1890	-0.3528	-0.3520	0.3520	0.3520
0.10	0.7329	0.7327	0.2308	0.2289	-0.2743	-0.2743	-0.2453	-0.2445	0.3200	0.3200
0.14	0.8825	0.8823	0.3645	0.3619	-0.3303	-0.3302	-0.1480	-0.1472	0.2880	0.2880
0.18	0.9616	0.9615	0.5081	0.5047	-0.3599	-0.3599	-0.0610	-0.0601	0.2560	0.2560
0.22	0.9782	0.9781	0.6334	0.6495	-0.3662	-0.3661	0.0157	0.0166	0.1240	0.1240
0.26	0.9401	0.9400	0.7936	0.7892	-0.3519	-0.3518	0.0823	0.0831	0.1920	0.1920
0.30	0.8551	0.8550	0.9226	0.9177	-0.3201	-0.3200	0.1387	0.1395	0.1600	0.1600
0.34	0.7310	0.7309	1.0350	1.0300	-0.2736	-0.2736	0.1848	0.1856	0.1280	0.1280
0.38	0.5756	0.5755	1.1270	1.1210	-0.2154	-0.2154	0.2206	0.2214	0.0960	0.0960
0.42	0.3968	0.3967	1.1950	1.1890	-0.1485	-0.1485	0.2462	0.2470	0.0640	0.0640
0.46	0.2023	0.2023	1.2370	1.2310	-0.0757	-0.0757	0.2616	0.2624	0.0320	0.0320
0.50	0.0000	0.0000	1.2510	1.2450	0.0000	0.0000	0.2667	0.2675	0.0000	0.0000
0.54	-0.2023	-0.2023	1.2370	1.2310	0.0757	0.0757	0.2616	0.2624	-0.0320	-0.0320
0.58	-0.3968	-0.3967	1.1950	1.1890	0.1485	0.1485	0.2462	0.2470	-0.0640	-0.0640
0.62	-0.5756	-0.5755	1.1270	1.112	0.2154	0.2154	0.2206	0.2214	-0.0960	-0.0960
0.66	-0.7310	-0.7309	1.0350	1.030	0.2736	0.2736	0.1848	0.1856	-0.1280	-0.1280
0.70	-0.8551	-0.8550	0.9226	0.9177	0.3201	0.3200	0.1387	0.1395	-0.1600	-0.1600
0.74	-0.9401	-0.9400	0.7936	0.7892	0.3519	0.3518	0.0823	0.0831	-0.1920	-0.1920
0.78	-0.9782	-0.9781	0.6535	0.6495	0.3662	0.3661	0.0158	0.0166	-0.2240	-0.2240
0.82	-0.9616	-0.9615	0.5081	0.5047	0.3599	0.3599	-0.0609	-0.0601	-0.2560	-0.2560
0.86	-0.8825	-0.8823	0.3645	0.3619	0.3303	0.3302	-0.1480	-0.1472	-0.2880	-0.2880
0.90	-0.7329	-0.7328	0.2308	0.2289	0.2743	0.2743	-0.2453	-0.2445	-0.3200	-0.3200
0.94	-0.5052	-0.5050	0.1158	0.1147	0.1891	0.1890	-0.3528	-0.3520	-0.3520	-0.3520
0.98	-0.1915	-0.1913	0.0292	0.0291	0.0716	0.0716	-0.4706	-0.4698	-0.3840	-0.3840
1.00	0.0000	0.0000	0.0000	0.0000	0.0000	0.0000	-0.5333	-0.5325	-0.4000	-0.4000

* CF denotes closed-form solutions; TM signifies transfer-matrix solution.

Table 7. Comparison between closed-form and transfer-matrix solutions for an aramid-cord rubber beam (Case 4)

x/l	$u \times 10^3$, in		$w \times 10^2$, in		$\psi \times 10^3$, rad		$M \times 10^6$, lb-in		$Q \times 10^6$, lb	
	CF*	TM*	CF*	TM*	CF*	TM*	CF*	TM*	CF*	TM*
0.00	0.00000	0.00000	0.00000	0.00000	-0.00000	0.00000	-1.4360	-1.4300	1.6320	1.6310
0.02	0.0498	0.0496	0.0112	0.0111	-0.1865	-0.1857	-1.1750	-1.1700	1.6220	1.6210
0.06	0.1200	0.1195	0.0407	0.0401	-0.4401	-0.4474	-0.6667	-0.6616	1.5430	1.5410
0.10	0.1526	0.1521	0.0750	0.0739	-0.5711	-0.5692	-0.1957	-0.1910	1.3890	1.3880
0.14	0.1514	0.1510	0.1088	0.1073	-0.5666	-0.5652	0.2154	0.2196	1.1710	1.1690
0.18	0.1217	0.1216	0.1378	0.1359	-0.4555	-0.4550	0.5480	0.5517	0.9011	0.8996
0.22	0.0700	0.0702	0.1585	0.1564	-0.2622	-0.2630	0.7884	0.7917	0.5975	0.5961
0.26	0.0038	0.004494	0.1682	0.1660	-0.0144	-0.0168	0.9288	0.9316	0.2790	0.2776
0.30	-0.0691	-0.06809	0.1658	0.1637	0.2589	0.2649	0.9675	0.9699	-0.0345	-0.0359
0.34	-0.1414	-0.1399	0.1510	0.1491	0.5293	0.5236	0.9093	0.9112	-0.3233	-0.3247
0.38	-0.2058	-0.2039	0.1247	0.1231	0.7704	0.7634	0.7652	0.7666	-0.5692	-0.5707
0.42	-0.2565	-0.2543	0.0888	0.0877	0.0877	0.0958	0.5513	0.5523	-0.7568	-0.7582
0.46	-0.2888	-0.2864	0.0462	0.0456	1.0810	1.0720	0.2883	0.2888	-0.8743	-0.8757
0.50	-0.2998	-0.2974	0.0001	0.0001	1.1220	1.1130	0.0009	0.0009	-0.9143	-0.9157
0.54	0.2888	0.2864	-0.0462	-0.0456	1.0810	1.0720	-0.2883	-0.2887	-0.8743	-0.8757
0.58	0.2565	0.2543	-0.0888	-0.0877	0.9600	0.9518	-0.5513	-0.5521	-0.7568	-0.7583
0.62	0.2058	0.2039	-0.1247	-0.1231	0.7704	0.7634	-0.7652	-0.7665	-0.5692	-0.5707
0.66	0.1414	0.1399	-0.1510	-0.1491	0.5293	0.5236	-0.9093	-0.9111	-0.3233	-0.3247
0.70	0.0691	0.0680	-0.1658	-0.1637	0.2589	0.2549	-0.9675	-0.9697	-0.0345	-0.0359
0.74	-0.0038	-0.0044	-0.1682	-0.1660	-0.0144	-0.0168	-0.9288	-0.9315	0.2790	0.2775
0.78	-0.0700	-0.0702	-0.1585	-0.1564	-0.2622	-0.2630	-0.7884	-0.7916	0.5975	0.5961
0.82	-0.1217	-0.1215	-0.1378	-0.1359	-0.4555	-0.4550	-0.5480	-0.5516	0.9011	0.8996
0.86	-0.1514	-0.1510	-0.1088	-0.1073	-0.5666	-0.5652	-0.2154	-0.2195	1.1710	1.1690
0.90	-0.1526	-0.1521	-0.0749	-0.0738	-0.5711	-0.5692	0.1957	0.1912	1.3890	1.3880
0.94	-0.1200	-0.1195	-0.0407	-0.0401	-0.4491	-0.4474	0.6667	0.6617	1.5430	1.5410
0.98	-0.0498	-0.4962	-0.0112	-0.0111	-0.1865	-0.1857	1.1750	1.1710	1.6220	1.6210
1.00	0.0000	0.0000	0.0000	0.0000	0.0000	0.0000	1.4360	1.4300	1.6320	1.6310

* CF denotes closed-form solutions; TM signifies transfer-matrix solution.

Table 8. Forces, displacements, and neutral-surface positions
of an aramid-cord rubber beam (Case 5), as analyzed
using the transfer-matrix method*

x/ℓ	$u \times 10$, in	w , in	$\psi \times 10$, in	M , lb-in	q , lb	z_n , in
0.00	1.0000	0.0000	0.0000	-2.5000	0.7000	0.2695
0.02	-0.0104	0.0007	-0.0387	-2.3890	0.6840	0.2695
0.06	-0.0300	0.0039	-0.1116	-2.1760	0.6520	0.2698
0.10	-0.0481	0.0093	-0.1785	-1.9720	0.6200	0.2701
0.14	-0.0646	0.0167	-0.2397	-1.7790	0.5880	0.2703
0.18	-0.0798	0.0259	-0.2956	-1.5960	0.5560	0.2707
0.22	-0.0935	0.0369	-0.3463	-1.4230	0.5240	0.2711
0.26	-0.1060	0.0493	-0.3923	-1.2600	0.4920	0.2715
0.30	-0.1173	0.0631	-0.4338	-1.1080	0.4600	0.2720
0.34	-0.1274	0.0781	-0.4710	-0.9659	0.4280	0.2726
0.38	-0.1365	0.0942	-0.5044	-0.8341	0.3960	0.2734
0.42	-0.1447	0.1113	-0.5341	-0.7125	0.3640	0.2742
0.46	-0.1519	0.1292	-0.5605	-0.6011	0.3320	0.2753
0.50	-0.1584	0.1478	-0.5838	-0.5003	0.3001	0.2765
0.54	-0.1641	0.1673	-0.6045	-0.4091	0.2680	0.2781
0.58	-0.1691	0.1872	-0.6226	-0.3285	0.2360	0.2799
0.62	-0.1736	0.2076	-0.6386	-0.2581	0.2040	0.2823
0.66	-0.1776	0.2285	-0.6527	-0.1979	0.1720	0.2853
0.70	-0.1812	0.2498	-0.6652	-0.1480	0.1400	0.2892
0.74	-0.1845	0.2714	-0.6764	-0.1083	0.1080	0.2955
0.78	-0.1875	0.2953	-0.6860	-0.0788	0.0760	0.3803
0.82	-0.1905	0.3154	-0.6930	-0.0596	0.0440	0.5027
0.86	-0.1937	0.3377	-0.6987	-0.0507	0.0120	0.5915
0.90	-0.1967	0.3602	-0.7039	-0.0520	-0.0200	0.5769
0.94	-0.1998	0.3828	-0.7098	-0.0635	-0.0520	0.4723
0.98	-0.2029	0.4055	-0.7174	-0.0852	-0.0840	0.3518
1.00	-0.2044	0.4170	-0.7221	-0.01000	-0.1000	0.3000

* $N_1 = -1.000$ lb (compressive)

Table 9. Forces, displacements, and neutral-surface positions
of an aramid-cord rubber beam (Case 6), as analyzed
using the transfer-matrix method*

x/l	$u \times 10, \text{in}$	w, in	$\psi \times 10, \text{rad}$	$M, \text{lb-in}$	Q, lb	z_n, in
0.00	-0.0000	-0.0000	0.0000	1.7190	-0.1000	-0.2631
0.02	-0.0054	-0.0002	0.0206	1.7030	-0.1010	-0.2631
0.06	-0.01609	-0.0016	0.0611	1.6690	-0.1085	-0.2630
0.10	-0.02649	-0.0043	0.1007	1.6320	-0.1243	-0.2629
0.14	-0.03658	-0.0083	0.1391	1.5890	-0.1462	-0.2627
0.18	-0.04631	-0.0136	0.1761	1.5380	-0.1731	-0.2626
0.22	-0.05561	-0.0200	0.2116	1.4780	-0.2035	-0.2624
0.26	-0.06442	-0.0276	0.2452	1.4080	-0.2353	-0.2621
0.30	-0.07266	-0.0362	0.2766	1.3270	-0.2667	-0.2617
0.34	-0.0824	-0.0459	0.3056	1.2370	-0.2955	-0.2613
0.38	-0.08711	-0.0564	0.3320	1.1390	-0.3201	-0.2600
0.42	-0.09320	-0.0678	0.3554	1.0330	-0.3389	-0.2598
0.46	-0.09847	-0.0799	0.3757	0.9224	-0.3506	-0.2587
0.50	-0.1029	-0.0926	0.3927	0.8096	-0.3546	-0.2572
0.54	-0.1092	-0.1195	0.4174	0.5857	-0.3389	-0.2513
0.62	-0.1111	-0.1334	0.4250	0.4801	-0.3201	-0.2452
0.66	-0.1122	-0.1474	0.4298	0.3814	-0.2955	-0.2322
0.70	-0.1127	-0.1615	0.4319	0.2914	-0.2667	-0.1896
0.74	-0.1127	-0.1757	0.4323	0.2110	-0.2353	-0.0272
0.78	-0.1127	-0.1898	0.4324	0.1408	-0.2035	-0.1777
0.82	-0.1127	-0.2038	0.4325	0.0806	-0.1731	-0.3719
0.86	-0.1127	-0.2179	0.4325	0.0296	-0.1462	-1.0100
0.90	-0.1096	-0.2319	0.4333	-0.0134	-0.1243	2.2340
0.94	-0.1066	-0.2458	0.4300	-0.0505	-0.1089	0.5933
0.98	-0.1035	-0.2596	0.4232	-0.0839	-0.1010	0.3574
1.00	-0.1020	-0.2664	0.4185	-0.1000	-0.1000	0.3000

* $N_1 = -1.000 \text{ lb (compressive)}$

Table 10. Forces, displacements, and neutral-surface positions
of an aramid-cord rubber beam (Case 7), as analyzed
using the transfer-matrix method

x/ℓ	$u \times 10^3$, in	$w \times 10$, in	$\psi \times 10^2$, rad	$M, \text{lb-in}$	Q, lb	z_n , in
0.00	0.0000	0.0000	-0.3376	-0.1000	0.4000	0.5114
0.02	-0.2612	0.0080	-0.3727	-0.0372	0.3840	1.3720
0.06	-0.7835	0.0239	-0.3506	0.0804	0.3520	0.6355
0.10	-0.7853	0.0392	-0.3502	0.1880	0.3200	0.2692
0.14	-0.7870	0.0540	-0.3493	0.2853	0.2880	0.0990
0.18	-0.7875	0.0684	-0.3473	0.3723	0.2560	-0.0475
0.22	-0.7816	0.0822	-0.3416	0.4491	0.2240	-0.1518
0.26	-0.7537	0.0954	-0.3262	0.5157	0.1920	-0.1994
0.30	-0.6918	0.1075	-0.2968	0.5720	0.1600	-0.2185
0.34	-0.5966	0.1181	-0.2542	0.6181	0.1280	-0.2276
0.38	-0.4730	0.1267	-0.2005	0.6539	0.0960	-0.2326
0.42	-0.3276	0.1330	-0.1384	0.6795	0.0640	-0.2355
0.46	-0.1675	0.1370	-0.0706	0.6949	0.0320	-0.2370
0.50	0.0005	0.1383	0.0002	0.7000	0.000	-0.2384
0.54	0.1675	0.1370	0.0706	0.6949	-0.0320	-0.2370
0.58	0.3276	0.1330	0.1384	0.6795	-0.0640	-0.2355
0.62	0.4730	0.1267	0.2005	0.6539	-0.0960	-0.2326
0.66	0.5966	0.1181	0.2542	0.6181	-0.1280	-0.2276
0.70	0.6919	0.1075	0.2968	0.5720	-0.1600	-0.2185
0.74	0.7537	0.0954	0.3262	0.5157	-0.1920	-0.1994
0.78	0.7816	0.0822	0.3416	0.4491	-0.2240	-0.1518
0.82	0.7875	0.0684	0.3472	0.3723	-0.2560	-0.0475
0.86	0.7870	0.0540	0.3492	0.2853	-0.2880	0.0990
0.90	0.7853	0.0392	0.3501	0.1880	-0.3200	0.2692
0.94	0.7836	0.0239	0.3506	0.0804	-0.3520	0.6355
0.98	0.2612	0.0080	0.3727	-0.0372	-0.3840	1.3720
1.00	0.0	0.0	0.3376	-0.1000	-0.4000	0.5114

NOTE: Bending-stretching coupling caused by bimodulus action induces an axial force $N = -1.705 \text{ lb}$ (compressive).

Table II. Forces, displacements, and neutral-surface positions
of an aramid-cord rubber beam (Case 8), as analyzed
using the transfer-matrix method

x/ℓ	$u \times 10^3$, in	$w \times 10^4$, in	$\psi \times 10^2$, rad	$M, 1b\text{-in}$	$q, 1b$	z_n , in
0.00	0.0000	0.0000	-0.1137	-0.1000	0.1273	0.1251
0.02	-0.0002	0.0257	-0.1141	-0.0796	0.1263	-0.0066
0.06	0.0000	0.0769	-0.1144	-0.0403	0.1184	-0.2979
0.10	0.0004	0.1268	-0.1145	-0.0047	0.1030	-2.5490
0.14	0.0009	0.1744	-0.1144	0.0249	0.0811	-0.4822
0.18	0.1236	0.2132	-0.0778	0.0466	0.0542	-0.2936
0.22	0.2552	0.2355	-0.0326	0.0592	0.0238	-0.2892
0.26	0.3924	0.2393	0.0148	0.0617	-0.0089	-0.2886
0.30	0.5277	0.2243	0.0615	0.0541	-0.0393	-0.2907
0.34	0.6504	0.1907	0.1081	0.0358	-0.0682	-0.3257
0.38	0.7731	0.1426	0.1325	0.0109	-0.0928	-1.0940
0.42	0.8588	0.0834	0.1615	-0.0219	-0.1116	-0.5484
0.46	0.8592	0.0177	0.1613	-0.0596	-0.1233	-0.1532
0.50	-0.8592	-0.0485	0.1608	-0.0998	-0.1273	-0.1244
0.54	-0.8498	-0.1144	0.1559	-0.1403	-0.1233	-0.2240
0.58	-0.8138	-0.1758	0.1406	-0.1781	-0.1116	-0.2419
0.62	-0.7518	-0.2290	0.1154	-0.2110	-0.0928	-0.2484
0.66	-0.6679	-0.2701	0.0818	-0.2369	-0.0682	-0.2516
0.70	-0.5677	-0.2964	0.0421	-0.2542	-0.0393	-0.2531
0.74	-0.4581	-0.3058	0.0011	-0.2618	-0.0089	-0.2537
0.78	-0.3466	-0.2974	-0.0450	-0.2592	0.0239	-0.2535
0.82	-0.2408	-0.2716	-0.0868	-0.2467	0.0542	-0.2525
0.86	-0.1479	-0.2299	-0.1238	-0.2249	0.0811	-0.2503
0.90	-0.0743	-0.1745	-0.1534	-0.1953	0.1030	-0.2458
0.94	-0.0250	-0.1089	-0.1739	-0.1597	0.1184	-0.2355
0.98	-0.0025	-0.0371	-0.1839	-0.1203	0.1263	-0.1978
1.00	0.0000	0.0000	-0.1854	-0.1000	0.1273	0.1251

NOTE: Bending-stretching coupling caused by bimodulus action induces an axial force $N = -0.4004 \text{ lb}$ (compressive).

PART II

TRANSIENT RESPONSE OF A THICK BEAM
OF BIMODULAR MATERIAL

C.W. Bert
School of Aerospace, Mechanical and Nuclear Engineering
The University of Oklahoma
Norman, Oklahoma, U.S.A.

and

A.D. Tran
Exxon Production Research
Houston, Texas, U.S.A.

SUMMARY

Certain materials have different elastic behavior when they are loaded in tension as compared to compression. As an engineering approximation, they are usually modeled as a bimodular material, i.e., a bilinear material having different Young's moduli in tension and in compression. All of the previous analyses of bimodular beams known to the present investigators have been concerned with either static loading or harmonic vibration. Thus, the present work is believed to be the first to consider transient response of such beams. The transfer-matrix method is used to discretize spatially, while the timewise discretization is accomplished by use of the Newmark beta method.

INTRODUCTION

There is an extensive body of literature on the static behavior of bimodular beams, going back as far as Timoshenko in 1941.¹ These works were recently discussed in connection with a transfer-matrix static analysis of bimodular beams by the present investigators.² Examples of material having such behavior are cord-rubber, soft biological tissues, paperboard, and reinforced concrete.

The only dynamic analyses of bimodular beams known to the present investigators are the works of Khachatryan³ in 1967, Galoyan and Khachatryan⁴ in 1978, and Tran⁵ in 1981. All of these involved either free or sinusoidally forced vibrations.

The present work uses the transfer-matrix method⁶, which was shown in Ref. 2 to be both more accurate and computationally more efficient than the finite-element method for a statically loaded bimodular beam. The neutral-surface position, which is the boundary between the tensile and compressive regions of a cross section is permitted to vary in a piecewise linear fashion along the beam length. The beam is modeled as a Timoshenko beam, i.e.; both transverse shear deformation and rotatory inertia are considered.

Numerous approaches have been used to handle transient response problems; these have included various transform techniques⁷, the so-called direct-analysis method⁸, the modal method⁹, and various numerical-integration schemes. Among the latter are the central-difference method¹⁰, the Houbolt method¹¹, the Newmark beta method¹², the Wilson theta method¹³, and stiffly stable methods.¹⁴ For simplicity and efficiency, the present analysis uses the Newmark method.

GOVERNING EQUATIONS

A relatively thick rectangular-section beam of thickness h and length l is considered to be undergoing small-displacement motion. The x axis is located on the beam midplane and the z axis is directed downward normal to x .

The Timoshenko-beam-theory displacement field, as follows, is used:

$$\begin{aligned} U(x, z, t) &= u(x, t) + z\psi(x, t) \\ W(x, z, t) &= w(x, t) \end{aligned} \quad (1)$$

Here, U and W are the displacement components in the respective x and z directions, u and w are the corresponding midplane displacements, t is time, and ψ is the bending slope.

The axial and transverse stress resultants N and Q and stress couple M , each per unit width, are defined as

$$(N, Q) = \int_{-h/2}^{h/2} (\sigma_x, \tau_{xz}) dz \quad ; \quad M = \int_{-h/2}^{h/2} z\sigma_x dz \quad (2)$$

where σ_x and τ_{xz} are respectively the axial normal stress and the transverse shear stress.

Due to the bimodular action (different properties in tension and compression), bending-stretching coupling is induced in a straight beam of bimodular material even when it undergoes small deflections. Thus, the appropriate constitutive relation is reminiscent of that for a beam unsymmetrically laminated of ordinary (not bimodular) materials¹⁵:

$$\begin{Bmatrix} N \\ M \end{Bmatrix} = \begin{bmatrix} A & B \\ B & D \end{bmatrix} \begin{Bmatrix} \partial u / \partial x \\ \partial \psi / \partial x \end{Bmatrix} \quad (3)$$

$$Q = S[\psi + (\partial w / \partial x)]$$

The symbols A , B , D , and S denote the respective stretching, bending-stretching coupling, bending, and transverse shear stiffnesses, all per unit width, defined by

$$(A, B, D) = \int_{-h/2}^{h/2} Q^{(k)}(1, z, z^2) dz ; \quad S = K^2 \int_{-h/2}^{h/2} G dz \quad (4)$$

Here, G is the shear modulus in the xz plane; K^2 is the shear correction coefficient; $Q^{(k)}$ is $E_x^{(k)}$ for a compact-section beam or $E_x^{(k)} / (1 - v_{xy}^{(k)} v_{yx}^{(k)})$ for a wide beam; and $k = t$ for tensile-strain regions and $k = c$ for compressive regions.

The equations of motion appropriate for the subject beam are

$$\begin{aligned} \frac{\partial N}{\partial x} &= P \frac{\partial^2 u}{\partial t^2} \\ \frac{\partial Q}{\partial x} &= P \frac{\partial^2 w}{\partial t^2} - q(x, t) \\ \frac{\partial M}{\partial x} - Q &= I \frac{\partial^2 \psi}{\partial t^2} \end{aligned} \quad (5)$$

Here, $q(x, t)$ is the transverse distributed loading and P, I denote the respective transverse translatory and rotatory inertia coefficients per unit length:

$$(P, I) = \int_{-h/2}^{h/2} (1, z^2) dz \quad (6)$$

where ρ is the material density.

Equations (3) and (5) can be combined to obtain the following "displacement equations of motion":

$$\begin{aligned} \frac{\partial}{\partial x} (A \frac{\partial u}{\partial x} + B \frac{\partial \psi}{\partial x}) &= P \frac{\partial^2 u}{\partial t^2} \\ \frac{\partial}{\partial x} [S(\frac{\partial w}{\partial x} + \psi)] &= P \frac{\partial^2 w}{\partial t^2} - q(x, t) \\ \frac{\partial}{\partial x} (B \frac{\partial u}{\partial x} + D \frac{\partial \psi}{\partial x}) - S(\frac{\partial w}{\partial x} + \psi) &= I \frac{\partial^2 \psi}{\partial t^2} \end{aligned} \quad (7)$$

As demonstrated in Appendix A, in bimodular beams, the beam stiffnesses A, B, and D depend upon the neutral-surface position z_n , which is defined by setting the axial normal strain equal to zero:

$$\epsilon_x = \frac{\partial u}{\partial x} + z_n \frac{\partial \psi}{\partial x} = 0$$

Thus,

$$z_n = - \frac{\partial u / \partial \psi}{\partial x / \partial x} \quad (8)$$

TRANSFER-MATRIX FORMULATION

As a result of the present investigators' recent success in obtaining very accurate results for statically loaded, highly bimodular beams by using the transfer-matrix method², it was decided to use this spatial-discretization approach here. Briefly, the beam is divided into a number (N_s) of mass elements, each of which is assumed to have all of its mass concentrated at its mass center, the location of which is called a station. Consecutive stations are separated by massless fields containing all of the stiffnesses present in the system. Consequently, the complete beam is discretized to consist of two half fields ($\Delta x/2$), one at each end of the beam, and N_s stations separated by $N_s - 1$ full fields of length Δx . The role of the transfer matrix, which will be presented subsequently, is to transfer the generalized displacements (u, w, ψ) and the generalized forces (N, Q, M) from the left side of the field or station to the right side of the same field or station. For completeness, the field matrix for the present problem is given in Appendix B.

Following Chu and Pilkey⁹, we use the Newmark acceleration and velocity relations in the following form

$$\frac{\partial^2 y_{n+1}}{\partial t^2} = \frac{y_{n+1}}{3(\Delta t)^2} - \left[\frac{y_n}{3(\Delta t)^2} + \frac{\partial y_n / \partial t}{3\Delta t} + \left(\frac{1}{2\beta} - 1 \right) \frac{\partial^2 y_n}{\partial t^2} \right]$$

$$\frac{\partial y_{n+1}}{\partial t} = \frac{\partial y_n}{\partial t} + (1 - \lambda) \Delta t \frac{\partial^2 y_n}{\partial t^2} + \lambda \Delta t \frac{\partial^2 y_{n+1}}{\partial t^2} \quad (9)$$

Here, y denotes each of u , w , and ψ ; β and λ are coefficients; Δt is the time increment and the subscript $(n+1)$ denotes conditions at a time $(n+1)\Delta t$ with $n = 0, 1, 2, \dots$. As recommended in Ref. 9, we choose $\lambda = 1/2$ and $\beta \geq 1/4$.

Consideration of continuity at station i at time $(n+1)\Delta t$ enables one to write

$$(y_{n+1})_i^R = (y_{n+1})_i^L \quad (y = u, w, \psi) \quad (10)$$

After applying equations (9) to the time derivatives, one can write equations (7) in finite-difference form for station i at time $(n+1)\Delta t$ as

$$\begin{aligned} (N_{n+1})_i^R &= (N_{n+1})_i^L + P \left\{ \frac{(u_{n+1})_i^L}{\beta(\Delta t)^2} - \left[\frac{(u_n)_i^L}{\beta(\Delta t)^2} + \frac{1}{\beta \Delta t} \left(\frac{\partial u_n}{\partial t} \right)_i^L \right. \right. \\ &\quad \left. \left. + \left(\frac{1}{2\beta} - 1 \right) \left(\frac{\partial^2 u_n}{\partial t^2} \right)_i^L \right] \right\} \\ (Q_{n+1})_i^R &= (Q_{n+1})_i^L + P \left\{ \frac{(w_{n+1})_i^L}{\beta(\Delta t)^2} - \left[\frac{(w_n)_i^L}{\beta(\Delta t)^2} + \frac{1}{\beta \Delta t} \left(\frac{\partial w_n}{\partial t} \right)_i^L \right. \right. \\ &\quad \left. \left. + \left(\frac{1}{2\beta} - 1 \right) \left(\frac{\partial^2 w_n}{\partial t^2} \right)_i^L \right] \right\} - q(t) \quad (11) \\ (M_{n+1})_i^R &= (M_{n+1})_i^L + I \left\{ \frac{(\psi_{n+1})_i^L}{\beta(\Delta t)^2} - \left[\frac{(\psi_n)_i^L}{\beta(\Delta t)^2} + \frac{1}{\beta \Delta t} \left(\frac{\partial \psi_n}{\partial t} \right)_i^L \right. \right. \\ &\quad \left. \left. + \left(\frac{1}{2\beta} - 1 \right) \left(\frac{\partial^2 \psi_n}{\partial t^2} \right)_i^L \right] \right\} \end{aligned}$$

Equations (10) and (11) can be written in matrix notation as

$$\left\{ \begin{array}{c} u_{n+1} \\ w_{n+1} \\ \psi_{n+1} \\ M_{n+1} \\ Q_{n+1} \\ N_{n+1} \\ 1 \end{array} \right\}_i^R = \left[\begin{array}{ccccccc} 1 & 0 & 0 & 0 & 0 & 0 & 0 \\ 0 & 1 & 0 & 0 & 0 & 0 & 0 \\ 0 & 0 & 1 & 0 & 0 & 0 & 0 \\ 0 & 0 & I/3(\Delta t)^2 & 1 & 0 & 0 & -I\lambda_2 \\ 0 & P/(\Delta t)^2 & 0 & 0 & 1 & 0 & -P\lambda_3 \\ 0 & 0 & 0 & 0 & 0 & 0 & -P(\lambda_1 + \lambda_2) \\ 0 & 0 & 0 & 0 & 0 & 0 & 1 \end{array} \right] \left\{ \begin{array}{c} u_{n+1} \\ w_{n+1} \\ \psi_{n+1} \\ M_{n+1} \\ Q_{n+1} \\ N_{n+1} \\ 1 \end{array} \right\}_i^L \quad (12)$$

where

$$\begin{aligned} \lambda_1 &= \frac{(u_n)_i^L}{3(\Delta t)^2} + \frac{1}{3\Delta t} \left(\frac{\partial u_n}{\partial t} \right)_i^L + \left(\frac{1}{2\beta} - 1 \right) \left(\frac{\partial^2 u_n}{\partial t^2} \right)_i^L \\ \lambda_2 &= \frac{(\psi_n)_i^L}{3(\Delta t)^2} + \frac{1}{3\Delta t} \left(\frac{\partial \psi_n}{\partial t} \right)_i^L + \left(\frac{1}{2\beta} - 1 \right) \left(\frac{\partial^2 \psi_n}{\partial t^2} \right)_i^L \\ \lambda_3 &= \frac{(w_n)_i^L}{3(\Delta t)^2} + \frac{1}{3\Delta t} \left(\frac{\partial w_n}{\partial t} \right)_i^L + \left(\frac{1}{2\beta} - 1 \right) \left(\frac{\partial^2 w_n}{\partial t^2} \right)_i^L \end{aligned} \quad (13)$$

NUMERICAL RESULTS

Since no solution, analytical or numerical, is available for transient response of bimodular beams, the present transfer-matrix model could be checked only by comparison with results obtained for an ordinary-material beam. The comparison is made with a modal solution presented in Ref. 9. The material properties and dimensions of the beam are listed in Table I and the loading and boundary conditions are those of Case 1 in Table II. The tip-deflection response for 1-millisec time increments is shown in Figure 1. As can be seen, the agreement is close, thus serving as a benchmark validating the accuracy of the present transfer-matrix model as applied to transient analysis of beams.

The material and beam geometry selected for the bimodular problems investigated here were the same as those used in Ref. 2; see Table III. It is noted that this material is highly bimodular in nature, since $E_t/E_c \approx 300$.

Transient response of a clamped-clamped bimodular beam with axial constraint is investigated for loadings having different time functions and different spatial distributions. Load which is a step in time is investigated in Case 2 for uniform spatial distribution and in Case 3 for cosinusoidal spatial distribution. Load which is a ramp function in time is investigated in Cases 4 and 5 for uniform and cosinusoidal distribution. Maximum-deflection response with time for the above mentioned cases are illustrated in Figures 2 through 7. In all of these cases, oscillation keeps continuing without reducing amplitude, since the model developed in this study does not incorporate structural damping. However, the present model is still of value to designers since the predicted results are on the conservative side.

CONCLUDING REMARKS

In this study, a transfer-matrix model, based on Timoshenko-beam theory, was developed for a bimodular beam and applied to transient response problems. Since no transient response analyses of this type of beam by other methods of solution are presently available, it was not possible to make comparisons. However, for the case of a beam of ordinary material subjected to a triangular pulse, results obtained by the present method agreed well with those obtained by the modal method.

ACKNOWLEDGMENTS

The research reported here is based on a portion of the second author's thesis submitted in partial fulfillment of the requirements for the M.S. degree in Mechanical Engineering at the University of Oklahoma, May 1981. The authors acknowledge the University's Merrick Computing Center for providing computing time. The first author acknowledges the financial support of the Office of Naval Research, Structural Mechanical Program.

REFERENCES

1. S. Timoshenko, *Strength of Materials*, Part II: Advanced Theory and Problems, 2nd edn., Van Nostrand, Princeton, NJ, 1941, pp. 362-369.
2. A.D. Tran and C.W. Bert, 'Bending of thick beams of bimodulus materials', unpublished manuscript, 1981.
3. A.A. Khachatryan, 'Longitudinal vibrations of prismatic bars made of different-modulus materials,' *Mechanics of Solids* 2(5), 94-97 (1967).
4. A.G. Galoyan and A.A. Khachatryan, 'On transversal vibration of beams made from different modulus material' (in Russian), *Doklady Akademii Nauk Armyanskoi SSR* 66, 22-26 (1978). See *Applied Mechanics Reviews* 32, Rev. 10552 (1979).
5. A.D. Tran, 'Static and dynamic behavior of bimodulus beams,' unpublished M.S. thesis, Mechanical Engineering, The University of Oklahoma, Norman, OK, 1981.
6. F.A. Leckie and E. Pestel, 'Transfer matrix fundamentals,' *International Journal of Mechanical Sciences* 2, 137-167 (1960).
7. L.Y. Bahar, 'The use of integral transforms in the prediction of dynamic response,' *Shock and Vibration Digest* 5(9), 2-7 (1973).

8. H.A. Koenig and N. Davids, 'Dynamical finite element analysis for elastic waves in beams and plates,' *International Journal of Solids and Structures* 4, 643-660 (1968).
9. F.H. Chu and W.D. Pilkey, 'Transient analysis of structural members by the CSDT Riccati transfer matrix method, *Computers and Structures* 10, 500-611 (1979).
10. J.W. Leech, P.T. Hsu, and E.W. Mach, 'Stability of a finite-difference method for solving matrix equations,' *AIAA Journal* 3, 2172-2173 (1965).
11. J.C. Houbolt, 'A recurrence matrix solution for the dynamic response of elastic aircraft,' *Journal of the Aeronautical Sciences* 17, 540-550 (1950).
12. N.M. Newmark, 'A method of computation for structural dynamics,' *ASCE Journal of the Engineering Mechanics Division* 85(EM3), 67-94 (1959).
13. E.L. Wilson, 'A computer program for the dynamic stress analysis of underground structures,' SESM Report 68-1, Department of Civil Engineering, University of California, Berkeley, 1968.
14. P.S. Jensen, 'Stiffly stable methods for undamped second order equations of motion,' *SIAM Journal for Numerical Analysis* 13, 549-563 (1976).
15. Y.R. Kan and Y.M. Ito, 'Shear deformation in heterogeneous anisotropic plates,' *Journal of Composite Materials* 6, 316-319 (1972).

APPENDIX A: COMPUTATION OF BEAM STIFFNESSES FOR A BIMODULAR BEAM

The beam cross section is assumed to be compact and rectangular, extending from $z = -h/2$ to $z = h/2$. Since $E^{(k)}$ depends upon the sign of the axial strain, beam stiffnesses A, B, and D depend upon the neutral-surface position z_n , thus the first three of equations (4) must be integrated piecewise. For example, for concave upward bending ($\partial^2 w / \partial x^2 < 0$) the top portion of the cross section (from $-h/2$ to z_n) is in compression and the bottom portion (from z_n to $h/2$) is in tension. Thus, the first of equations (4) becomes

$$A = \int_{-h/2}^{z_n} E^c dz + \int_{z_n}^{h/2} E^t dz = [z_n + (h/2)]E^c + [(h/2) - z_n]E^t$$

or

$$A = (h/2)(E^t + E^c) - z_n(E^t - E^c)$$

In similar fashion

$$B = [(h^2/8) - (z_n^2/2)](E^t - E^c)$$

$$D = (h^3/24)(E^t + E^c) - (z_n^3/3)(E^t - E^c)$$

In the case of convex upward bending ($\partial^2 w / \partial x^2 > 0$), the results are:

$$A = (h/2)(E^t + E^c) + z_n(E^t - E^c)$$

$$B = -[(h^2/8) - (z_n^2/2)](E^t - E^c)$$

$$D = (h^3/24)(E^t + E^c) + (z_n^3/3)(E^t - E^c)$$

APPENDIX B: FIELD MATRIX FOR A THICK BEAM OF BIMODULAR MATERIAL

The following matrix equation was derived in Ref. 2:

$$\left\{ \begin{matrix} u \\ w \\ \psi \\ M \\ Q \\ N \\ 1 \end{matrix} \right\}^L = \left[\begin{matrix} 1 & 0 & 0 & \frac{B\Delta\ell}{\gamma} & \frac{B(\Delta\ell)^2}{2\gamma} & \frac{-D\Delta\ell}{\gamma} & \frac{-B\Delta\ell}{2\gamma} K_m \\ 0 & 1 & -A\ell & \frac{A(\Delta\ell)^2}{2\gamma} & \left[\frac{\Delta\ell}{S} + \frac{A(\Delta\ell)^3}{4\gamma} \right] & \frac{-B(\Delta\ell)^2}{2\gamma} & \frac{-A(\Delta\ell)^2}{4\gamma} K_m - \frac{\Delta\ell}{2S} K_q \\ 0 & 0 & 1 & \frac{-A\Delta\ell}{\gamma} & \frac{-A(\Delta\ell)^2}{2\gamma} & \frac{B\Delta\ell}{\gamma} & \frac{A\Delta\ell}{2\gamma} K_m \\ 0 & 0 & 0 & 1 & \Delta\ell & 0 & -K_m \\ 0 & 0 & 0 & 0 & 1 & 0 & -K_q \\ 0 & 0 & 0 & 0 & 0 & 1 & 0 \\ 0 & 0 & 0 & 0 & 0 & 0 & 1 \end{matrix} \right] \left\{ \begin{matrix} u \\ w \\ \psi \\ M \\ Q \\ N \\ 1 \end{matrix} \right\}^R$$

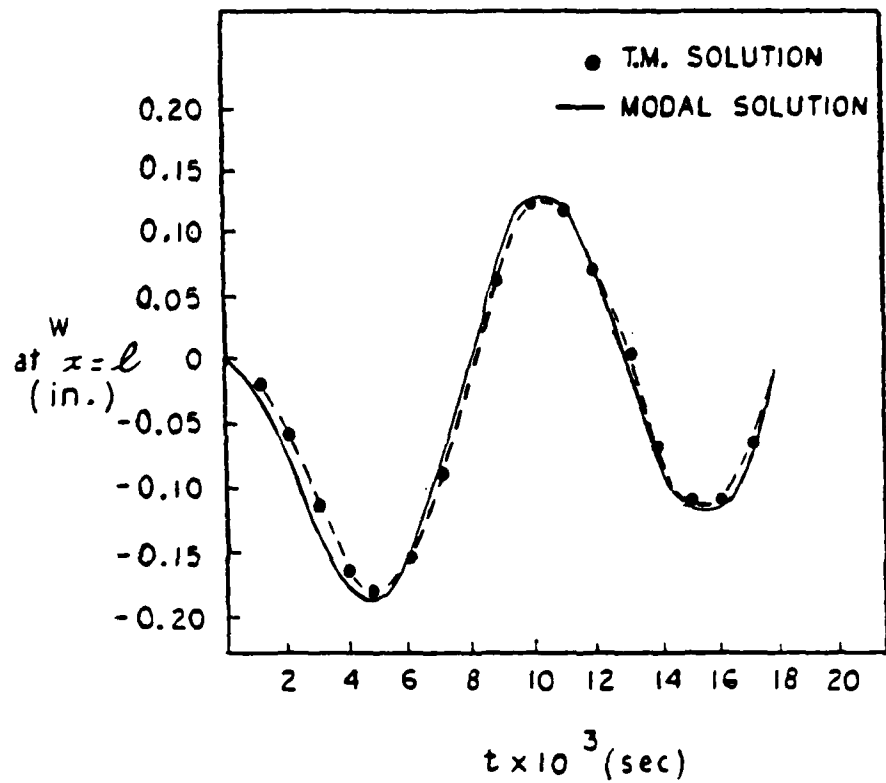


Figure 1. Comparison between transfer-matrix and modal solutions for a beam made of ordinary material and subjected to transient load (Case 1). Note: 1 in. = 2.54 cm.

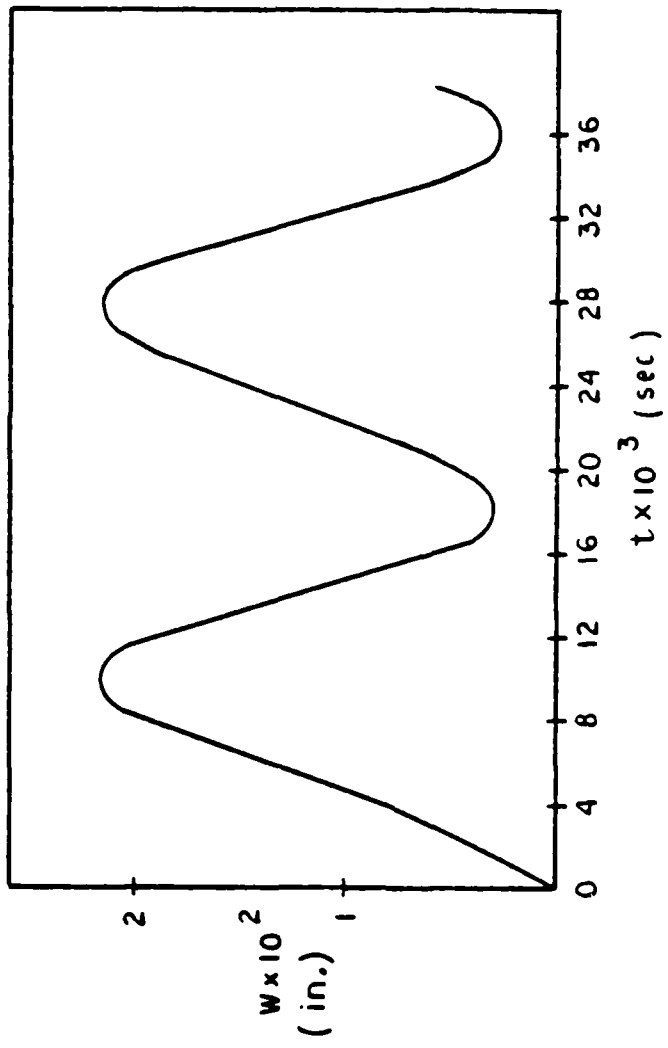


Figure 2. Maximum deflection (at $x = l/2$) versus time for a transiently loaded aramid-cord rubber beam (Case 2).
Note: 1 in. = 2.54 cm.

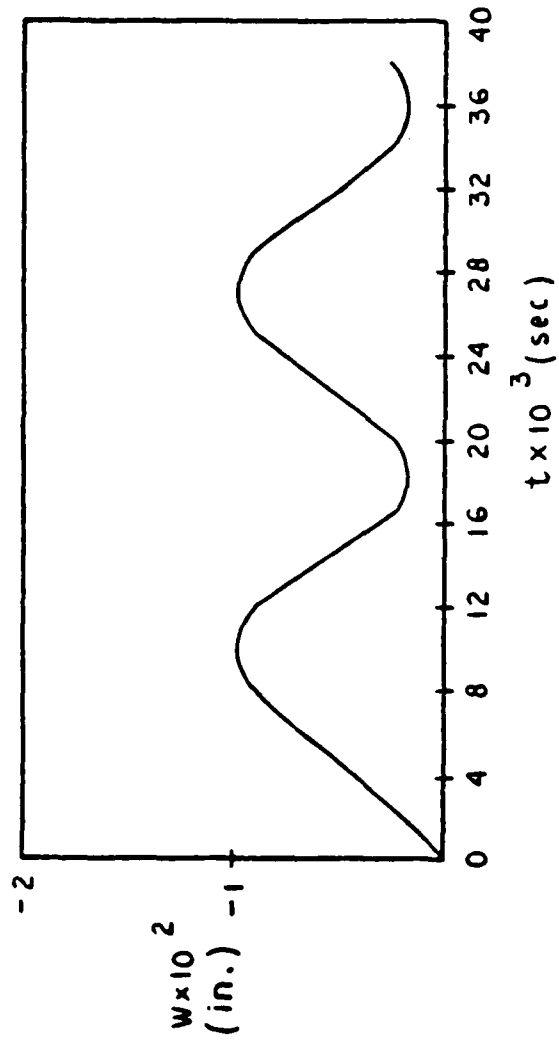


Figure 3. Maximum deflection (at $x = l/2$) versus time for a transiently loaded aramid-cord rubber beam (Case 3).
Note: 1 in. = 2.54 cm.

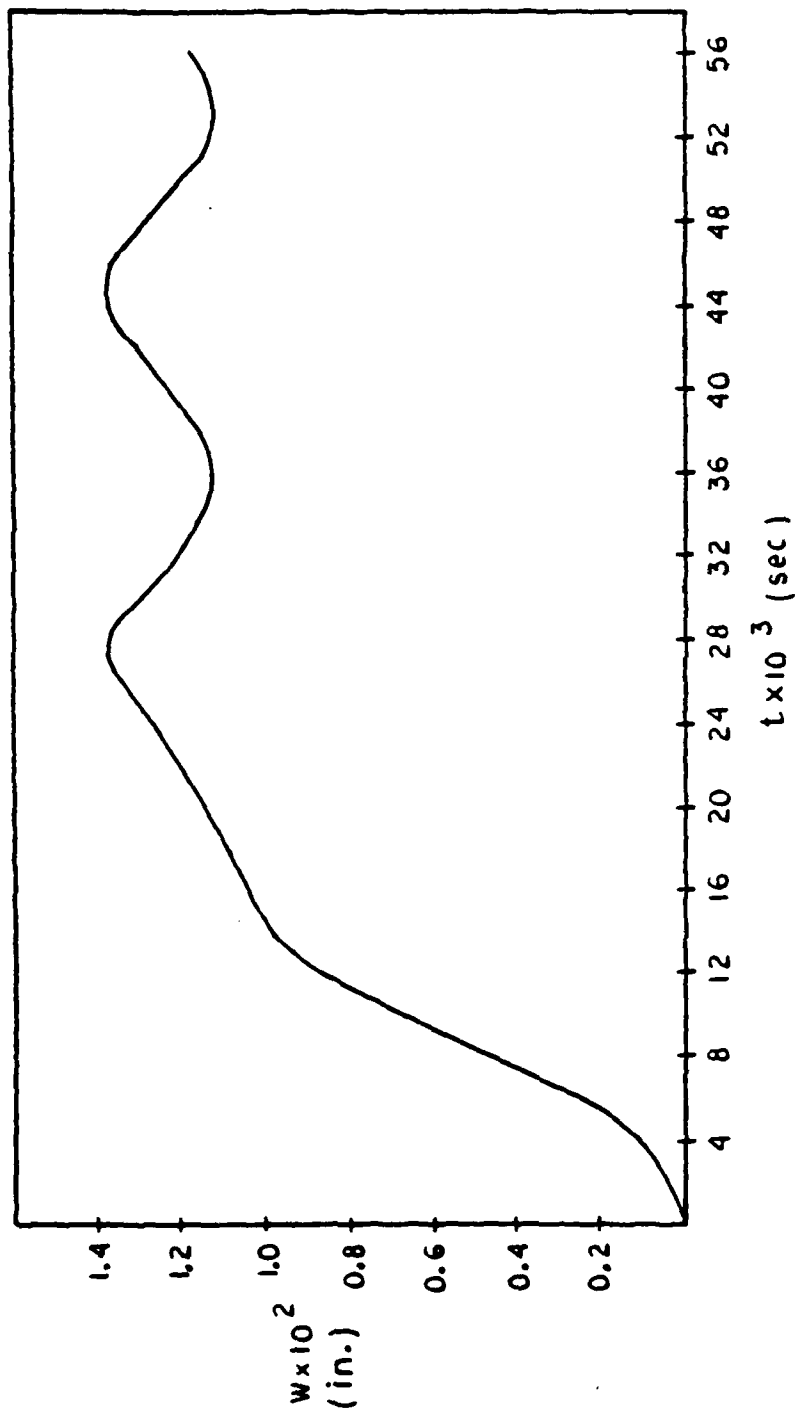


Figure 4. Maximum deflection (at $x = l/2$) versus time for a transiently loaded aramid-cord rubber beam (Case 4).
Note: 1 in. = 2.54 cm.

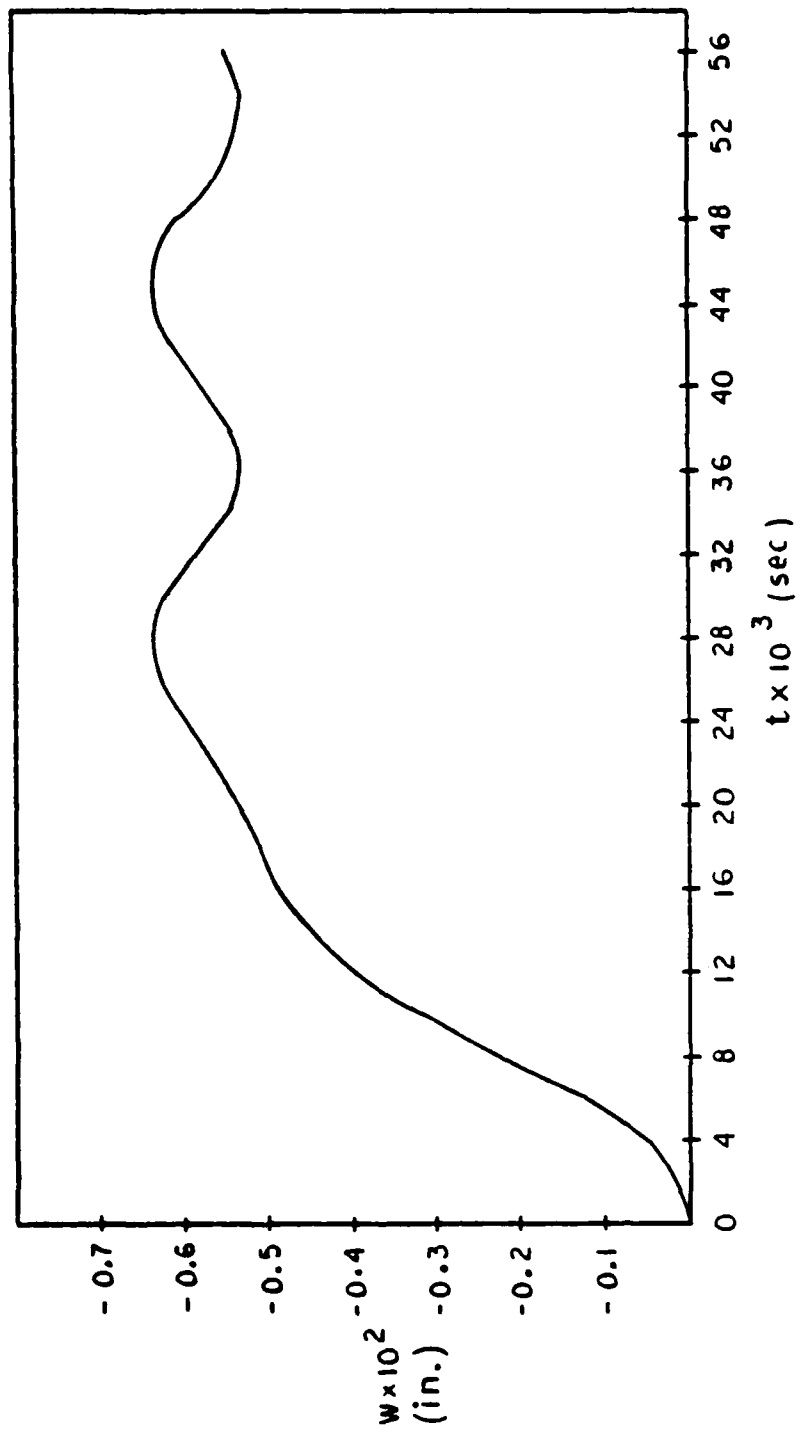


Figure 5. Maximum deflection (at $x = l/2$) versus time for a transiently loaded aramid-cord rubber beam (Case 5).
Note: 1 in. = 2.54 cm.

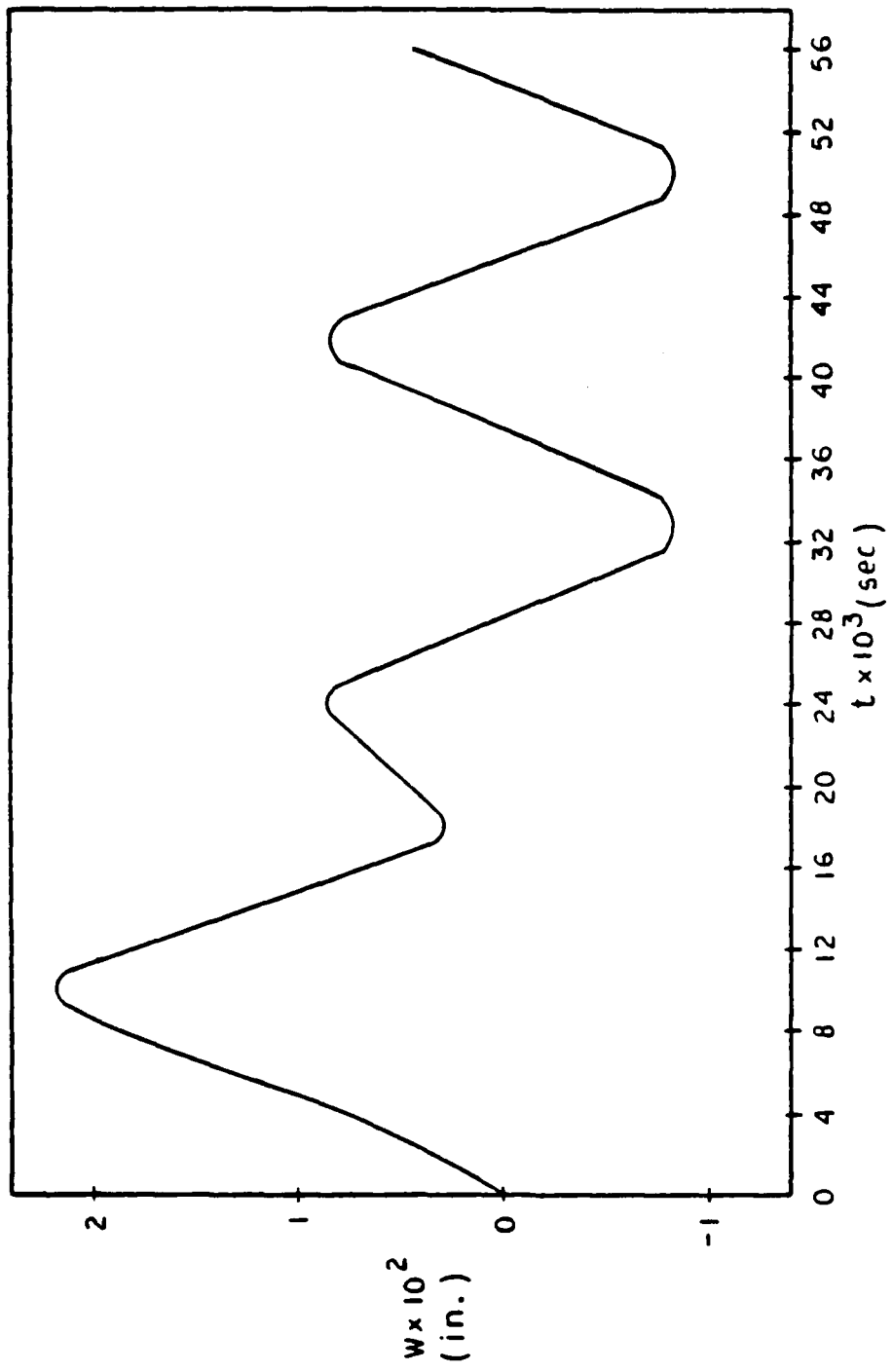


Figure 6. Maximum deflection at $(x = l/2)$ versus time for a transiently loaded aramid-cord rubber beam (Case 6).
Note: 1 in. = 2.54 cm.

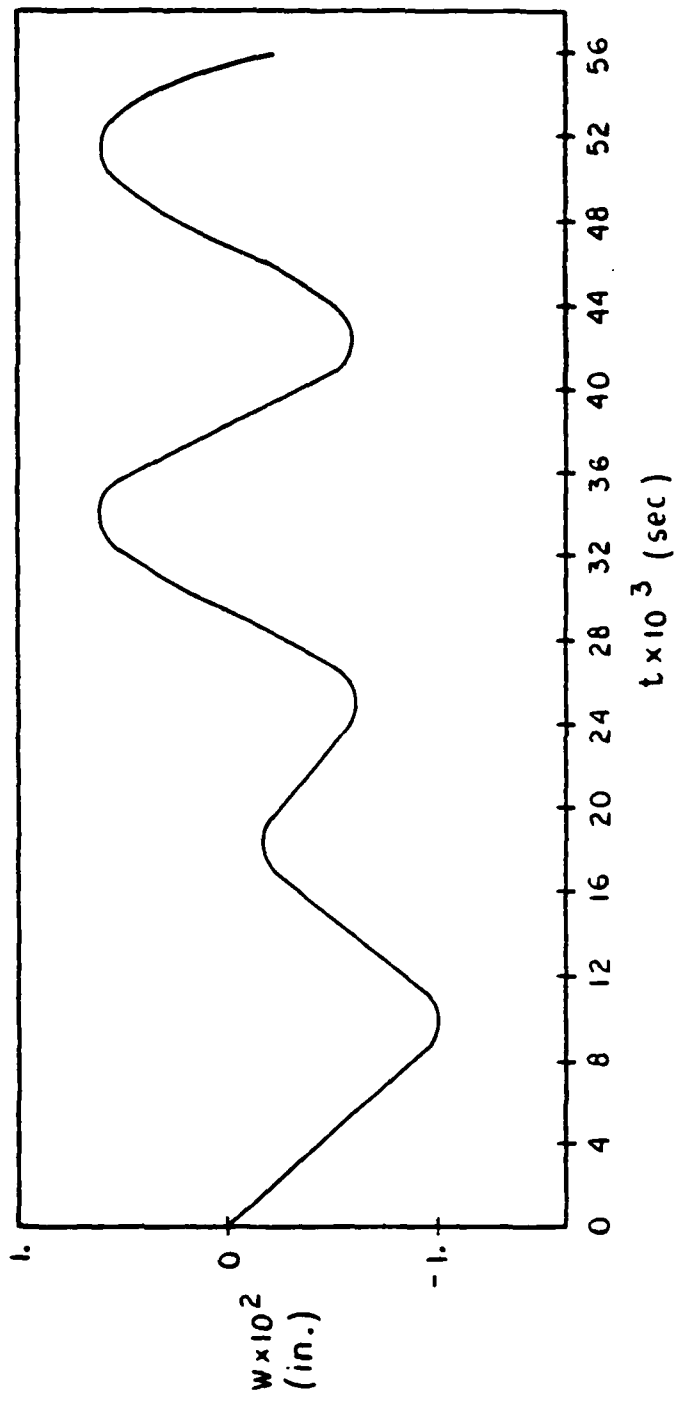


Figure 7. Maximum deflection at ($x = t/2$) versus time for a transiently loaded aramid-cord rubber beam (Case 7).
Note: 1 in. = 2.54 cm.

Table I. Material properties and beam dimensions for ordinary-material check problem

Property or Dimension	Value	
	SI units	English units
Material Properties:		
Young's modulus	207 GPa	30×10^6 psi
Shear modulus	79.6 GPa	11.5×10^6 psi
Specific gravity	8.20	8.20
Beam Dimensions:		
Length	183 cm	72.0 in.
Depth	58.7 cm	23.1 in.

Table II. Boundary conditions and spatial and temporal variations in loading considered

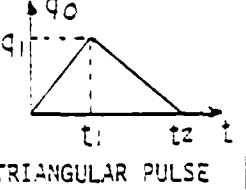
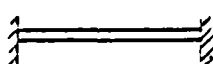
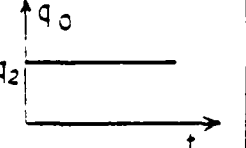
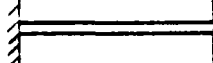
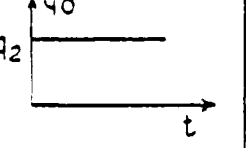
1	CLAMPED-FREE	$q = q_0$  $x=0$ $x=2$ UNIFORMLY DISTRIBUTED	 q ₀ q ₁ q ₂ t ₁ t ₂ t TRIANGULAR PULSE
2	CLAMPED-CLAMPED WITH AXIAL CONSTRAINT	$q = q_0$  $x=0$ $x=2$ UNIFORMLY DISTRIBUTED	 q ₀ q ₂ t STEP FUNCTION
3	CLAMPED-CLAMPED WITH AXIAL CONSTRAINT	$q = q_0 \cos \omega x$  COSINUSOIDAL ($\omega = 2\pi/2$)	 q ₀ q ₂ t STEP FUNCTION

Table II. (continued)

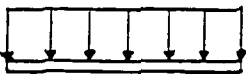
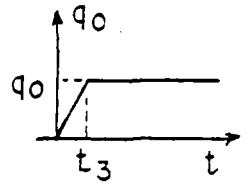
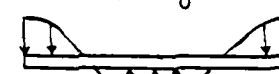
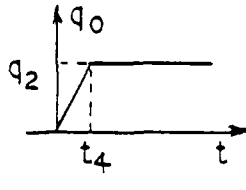
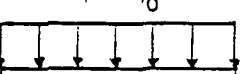
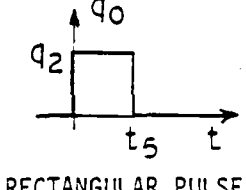
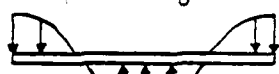
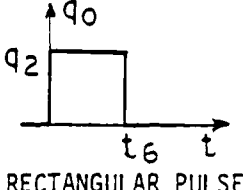
Case No.	Boundary conditions	Spatial distribution of distributed load	Time variation of distributed load
4	CLAMPED-CLAMPED WITH AXIAL CONSTRAINT	$q = q_0$  $x=0 \quad x=l$ UNIFORMLY DISTRIBUTED	 q_0 q_2 t_3 t
5	CLAMPED-CLAMPED WITH AXIAL CONSTRAINT	$q = q_0 \cos \alpha x$  $x=0 \quad x=l$ COSINUSOIDAL ($\alpha = 2\pi/l$)	 q_0 q_2 t_4 t
6	CLAMPED-CLAMPED WITH AXIAL RESTRAINT	$q = q_0$  $x=0 \quad x=l$ UNIFORMLY DISTRIBUTED	 q_0 q_2 t_5 t RECTANGULAR PULSE
7	CLAMPED-CLAMPED WITH AXIAL RESTRAINT	$q = q_0 \cos \alpha x$  $x=0 \quad x=l$ COSINUSOIDAL ($\alpha = 2\pi/l$)	 q_0 q_2 t_6 t RECTANGULAR PULSE

Table III. Material properties and beam dimensions
for aramid-cord rubber beam

Property or Dimension	Value	
	SI units	English units
Material Properties:		
Longitudinal Young's modulus in tension	3.58 GPa	519,300 psi
Longitudinal Young's modulus in compression	12.0 MPa	1,740 psi
Longitudinal-thickness shear modulus (independent of tension or compression)	3.70 MPa	537 psi
Specific gravity	1.02	1.02
Beam Dimensions:		
Length	20.3 cm	8.00 in.
Depth	1.52 cm	0.60 in.

PREVIOUS REPORTS ON THIS CONTRACT

Project Rept. No.	Issuing University Rept. No.*	Report Title	Author(s)
1	OU 79-7	Mathematical Modeling and Micromechanics of Fiber Reinforced Bimodulus Composite Material	C.W. Bert
2	OU 79-8	Analyses of Plates Constructed of Fiber-Reinforced Bimodulus Materials	J.N. Reddy and C.W. Bert
3	OU 79-9	Finite-Element Analyses of Laminated Composite-Material Plates	J.N. Reddy
4A	OU 79-10A	Analyses of Laminated Bimodulus Composite-Material Plates	C.W. Bert
5	OU 79-11	Recent Research in Composite and Sandwich Plate Dynamics	C.W. Bert
6	OU 79-14	A Penalty Plate-Bending Element for the Analysis of Laminated Anisotropic Composite Plates	J.N. Reddy
7	OU 79-18	Finite-Element Analysis of Laminated Bimodulus Composite-Material Plates	J.N. Reddy and W.C. Chao
8	OU 79-19	A Comparison of Closed-Form and Finite-Element Solutions of Thick Laminated Anisotropic Rectangular Plates (With a Study of the Effect of Reduced Integration on the Accuracy)	J.N. Reddy
9	OU 79-20	Effects of Shear Deformation and Anisotropy on the Thermal Bending of Layered Composite Plates	J.N. Reddy and Y.S. Hsu
10	OU 80-1	Analyses of Cross-Ply Rectangular Plates of Bimodulus Composite Material	V.S. Reddy and C.W. Bert
11	OU 80-2	Analyses of Thick Rectangular Plates Laminated of Bimodulus Composite Materials	C.W. Bert, J.N. Reddy, V.S. Reddy and W.C. Chao
12	OU 80-3	Cylindrical Shells of Bimodulus Composite Material	C.W. Bert and V.S. Reddy
13	OU 80-6	Vibration of Composite Structures	C.W. Bert
14	OU 80-7	Large Deflection and Large-Amplitude Free Vibrations of Laminated Composite-Material Plates	J.N. Reddy and W.C. Chao
15	OU 80-8	Vibration of Thick Rectangular Plates of Bimodulus Composite Material	C.W. Bert, J.N. Reddy, W.C. Chao, and V.S. Reddy
16	OU 80-9	Thermal Bending of Thick Rectangular Plates of Bimodulus Material	J.N. Reddy, C.W. Bert, Y.S. Hsu, and V.S. Reddy
17	OU 80-14	Thermoelasticity of Circular Cylindrical Shells Laminated of Bimodulus Composite Materials	Y.S. Hsu, J.N. Reddy, and C.W. Bert
18	OU 80-17	Composite Materials: A Survey of the Damping Capacity of Fiber-Reinforced Composites	C.W. Bert
19	OU 80-20	Vibration of Cylindrical Shells of Bimodulus Composite Materials	C.W. Bert and M. Kumar
20	VPI 81-11 & OU 81-1	On the Behavior of Plates Laminated of Bimodulus Composite Materials	J.N. Reddy and C.W. Bert
21	VPI 81-12	Analysis of Layered Composite Plates Accounting for Large Deflections and Transverse Shear Strains	J.N. Reddy

* OU denotes the University of Oklahoma; VPI denotes Virginia Polytechnic Institute and State University.

UNCLASSIFIED

SECURITY CLASSIFICATION OF THIS PAGE (When Data Entered)

REPORT DOCUMENTATION PAGE		READ INSTRUCTIONS BEFORE COMPLETING FORM
1. REPORT NUMBER OU-AMNE-81-7	2. GOVT ACCESSION NO. AD-A102 595	3. RECIPIENT'S CATALOG NUMBER
4. TITLE (and Subtitle) STATIC AND DYNAMIC ANALYSES OF THICK BEAMS OF BIMODULAR MATERIALS	5. TYPE OF REPORT & PERIOD COVERED Technical Report No. 22	
	6. PERFORMING ORG. REPORT NUMBER	
7. AUTHOR(s) Charles W. Bert and A.D. Tran	8. CONTRACT OR GRANT NUMBER(s) N00014-78-C-0647	
9. PERFORMING ORGANIZATION NAME AND ADDRESS School of Aerospace, Mechanical and Nuclear Engineering University of Oklahoma, Norman, OK 73019	10. PROGRAM ELEMENT, PROJECT, TASK AREA & WORK UNIT NUMBERS NR 064-609	
11. CONTROLLING OFFICE NAME AND ADDRESS Department of the Navy, Office of Naval Research Structural Mechanics Program (Code 474) Arlington, Virginia 22217	12. REPORT DATE July 1981	
	13. NUMBER OF PAGES 68	
14. MONITORING AGENCY NAME & ADDRESS (if different from Controlling Office)	15. SECURITY CLASS. (of this report) UNCLASSIFIED	
	15a. DECLASSIFICATION/DOWNGRADING SCHEDULE	
16. DISTRIBUTION STATEMENT (of this Report) This document has been approved for public release and sale; distribution unlimited.		
17. DISTRIBUTION STATEMENT (of the abstract entered in Block 20, if different from Report)		
18. SUPPLEMENTARY NOTES		
19. KEY WORDS (Continue on reverse side if necessary and identify by block number) Beams, bending-stretching coupling, bimodular materials, Newmark beta method, static bending, transverse shear deformation, Timoshenko beam theory, transfer-matrix method, transient response.		
20. ABSTRACT (Continue on reverse side if necessary and identify by block number) This report deals with the behavior of beams made of bimodular materials, which have one value for the elastic modulus in tension and another in com- pression. The transfer-matrix approach is used to investigate the small- deflection response to a variety of loadings, both static and transient. The beam is modeled as a Timoshenko beam, i.e., both transverse shear deforma- tion and rotatory inertia are included. Within each field element, provision is made for a neutral-surface position (locus of points having a zero value for the total axial normal strain) that may vary linearly with axial (over)		

UNCLASSIFIED

SECURITY CLASSIFICATION OF THIS PAGE(When Data Entered)

20. Abstract (Cont'd)

position within the element. The report consists of two distinct parts: Part I covers the static behavior, while Part II deals with transient dynamic behavior. In Part I, as a basis for comparative evaluation, exact closed-form solutions are also presented for special static cases in which the neutral-surface position is constant, i.e., independent of axial position. The results are also compared with finite-element results for one case. Agreement among all three methods is quite good. The treatment of the transient behavior in Part II is believed to be the first such analysis for bimodular beams. Timewise discretization is accomplished by use of the Newmark beta method. As an evaluation benchmark, the transient-analysis results obtained by applying the present transfer-matrix method to an ordinary-material (not bimodular) beam is compared with modal-analysis results with good agreement. Excitations considered include step, ramp, and rectangular pulse.

UNCLASSIFIED

SECURITY CLASSIFICATION OF THIS PAGE(When Data Entered)

